ISOLATION AND CHARACTERIZATION OF LIPID RAFTS IN *EMILIANIA HUXLEYI*: KEY PLAYERS IN HOST-VIRUS INTERACTIONS

by

SUZANNE L. ROSE

A thesis submitted to the

Graduate School-New Brunswick

Rutgers, The State University of New Jersey

in partial fulfillment of the requirements

for the degree of

Master of Science

Graduate Program in Ecology and Evolution

written under the direction of

Dr. Kay D. Bidle

and approved by

_____

_____

_____

_____

New Brunswick, New Jersey

January, 2013

ABSTRACT OF THE THESIS

Isolation and characterization of lipid rafts in *Emiliania huxleyi*: key players in host-virus interactions

By SUZANNE L. ROSE

Thesis Advisor:
Dr. Kay D. Bidle

Coccolithoviruses (EhVs) employ a suite of glycosphingolipids (GSLs) to successfully infect the globally important coccolithophore *Emiliania huxleyi*. Given their enrichment in glycosphingolipids and their involvement in sensing extracellular stimuli and activating signaling cascades through protein-protein interactions, lipid rafts and associated microdomains likely play a heretofore unappreciated role in viral infectivity and resistance mechanisms. Indeed, the lipid raft protein flotillin carries an evolutionary conserved prohibitin homology (PHB) domain, which has been shown to influence pathogen resistance by inducing hypersensitive response and cell death. Little to nothing is known about lipid rafts in unicellular photoautotrophic organisms, especially those from the marine environment. We combined bioinformatics, detergent treatment, density gradient purification, western blotting, lipidomics and genome-enabled proteomics to isolate and characterize the lipid and protein content of lipid rafts from control and EhV86-infected *E. huxleyi* strain CCMP1516.

Using bioinformatic analysis, we identified a flotillin-like protein (Protein ID 363433) in the *E. huxleyi* CCMP1516 genome, which contained several evolutionary-conserved features of known flotillin proteins. Western blot analysis further revealed immunoreactivity of a 67 kDa protein in *E. huxleyi* cell extracts to a human anti-flotillin antibody, consistent with the dimerized form of this protein and thereby providing a biochemical marker for lipid raft isolation. Lipid raft-enriched fractions were isolated and purified as detergent (Brij96) resistant membranes (DRMs) in Optiprep density gradients and their lipid and protein composition were subsequently characterized. TSQ mass spectrometry of the lipids in DRM fractions showed novel host-derived GSLs which co-purified with flotillin immunoreactive fractions. These fractions also contained notable vesicle morphology as confirmed by TEM.

Subsequent analysis of lipid raft proteome in both uninfected and EhV86-infected *E. huxleyi* cells collected at 2 h confirmed flotillin as one of the major proteins and more broadly provided key insight into host defense and virus infection strategies at the interface of lipid rafts and stress, programmed cell death, and innate immunity pathways. In particular, the detection of an EhV86-encoded C-type lectin (CTL)-containing protein (ehv149), with putative roles in cell adhesion and pathogen recognition receptors, suggests that EhV86 infection of *E. huxleyi* occurs by way of the recognition of specific glycosphingolipids and raft-associated proteins.

Acknowledgement

I would like to thank Dr. Kay Bidle for support and direction of this research, Dr. Chris Brown for help with protocol design and valuable discussions, Liti Haramaty for laboratory assistance, Frank Natale for flow cytometry assistance as well as the rest of Bidle lab family. I would also like to thank Dr. B.S. Van Mooy and Dr. Dr. Jamey Fulton, Woods Hole Oceanographic Institution, for the extensive lipidomic work and analytical discussions and Valentin Starvoytov for TEM analysis. This work was supported by NSF Grants OCE-0927829 and OCE-1061883 to K.D.B.

Table of Contents

Lists of Tables

List of Figures

1.0 Isolation and characterization of lipid rafts in *Emiliania huxleyi*: key players in host-virus interactions

1.1 Introduction

The coccolithophore *Emiliania huxleyi* (Lohmann) Hay &Mohler (Prymnesiophyceae, Haptophyta) forms massive spring blooms in the North Atlantic that are routinely infected and terminated by lytic, double-stranded DNA containing Coccolithoviruses (EhVs) (Bratbak, Egge et al. 1993; Jordan and Chamberlain 1997; Thierstein and Young 2004; Allen, Schroeder et al. 2006). As members of the Phycodnaviridae, EhVs are giant microalgal viruses (diameter ~180 nm) with an extensive genetic capability (~407 kb genomes) to manipulate host metabolic pathways for their replication (Castberg, Thyrhaug et al. 2002; Schroeder, Oke et al. 2002; Van Etten 2002; Wilson, Schroeder et al. 2005). Given the array of sensitive and resistant host strains in culture along with a number of genetically diverse EhVs, the *E. huxleyi*-EhV host-virus system has emerged as one of the best model systems to investigate host-virus interactions and the cellular processes mediating infection dynamics (Dassow, Ogata et al. 2009; Mackinder, Worthy et al. 2009; Bidle and Vardi 2011).

The determinants of host susceptibility or resistance to viral infection, along with the factors involved in the initial cellular response, are of fundamental interest in host-virus interactions. *Coccolithophores* employ a sophisticated, co-evolutionary biochemical "arms race" to manipulate host lipid metabolism and regulate cell fate via PCD, in a manner reminiscent of the 'Red Queen' dynamic (Van Valen 1973) driving plant- and animal-pathogen interactions (Staskawicz, Mudgett et al. 2001). Furthermore,

subtle differences in the physiological regulation of the PCD machinery appear to be critical in host susceptibility, perhaps as part of an innate immune repsonse to determine cell fate (Bidle and Kwityn 2012). Yet, very little is known about the cellular determinants of resistance/sensitivity and the interactions with host cell membranes.

The cell membrane fluid mosaic model proposed in 1972 by Singer and Nicolson has undergone rapid evolution over the past decade leading to the contemporary characterization of biological membranes as having discrete organizational regions – microdomains (Brown and London 2000; Edidin 2003; Lingwood and Simons 2010). Coined as "lipid rafts", these microdomains are enriched in sphingolipids, glycosphingolipids (GSLs) and sterols forming a liquid-ordered phase distinct from the phospholipid containing liquid-disordered phase of the surrounding membrane (Van Meer and Simons 1988; Rajendran and Simons 2005; Hancock 2006; Hakomori 2008). The biochemical nature of lipid rafts allows for their isolation due to their insolubility in cold non-ionic detergents (e.g. Brij-96 and Triton-X) and ability to form "detergent resistant membranes" (DRMs) (Radeva and Sharom 2004; Borner, Sherrier et al. 2005). Current data suggests lipid raft domain size having an average diameter of ~150 – 250 nm (Pike 2003), but it has been suggested that rafts begin as ~50 nm diameter assemblies that coalesce during varying cellular conditions (Simons and Ehehalt 2002).

The ability of lipid rafts to incorporate or exclude specific proteins and facilitate selective protein-protein interactions provide an important platform for the regulation of a wide range of cellular processes, including cytoskeleton organization, cell adhesion, signal transduction pathways, and apoptosis (Brown and London 2000; Munro 2003; Morrow and Parton 2005; Hancock 2006; Lingwood and Simons 2010). Small individual

lipid raft size (~10 - ~50 nm) suggests their role in the regulation of raft-associated proteins, whereby signaling proteins are physically separated and thereby held in an unactivated state (Simons and Ehehalt 2002). Subsequent clustering of lipid rafts into a larger platform (~200 nm) in turn enables protein-protein interactions essential to trigger pathways involved in cell growth, stress response, death, and survival (Simons and Ehehalt 2002). Lipid rafts have been found to be enriched in glycosylphosphatidylinositol (GPI)-anchored proteins, Src family kinases, heterotrimeric G proteins and Stomatin, prohibitin, flotillin and HflC/K (SPFH) superfamily proteins all of which are targeted to lipid rafts via essential lipid modification (Morrow and Parton 2005; Rajendran and Simons 2005; Rivera-Milla, Struermer et al. 2006). Flotillin, an evolutionary conserved SPFH domain-containing protein, has been proposed to function as a lipid raft organizer, acting as a scaffold and linking the aforementioned lipid raft domains and raft-dependent cellular process (Simons and Toomre 2000; Langhorst, Reuter et al. 2005; Morrow and Parton 2005). Flotillin-enriched lipid rafts appear to be involved in host invasion indicating a possibly important role in host-pathogen sensitivity or resistance (Rivera-Milla, Struermer et al. 2006; Babuke and Tikkanen 2007; del Cacho, Gallego et al. 2007).

Lipid rafts are targeted and usurped by a vast number of pathogens as sites of host attack in higher eukaryotes (van der Goot and Harder 2001). In the *E. huxleyi*-EhV system, they may function as specific points of viral attachment and entry, as well as in virus assembly and budding (Mackinder, Worthy et al. 2009; Bidle and Vardi 2011). *Coccolithoviruses* induce and employ a unique suite of virally encoded GSLs (vGSLs) to successfully infect *E. Huxleyi* (Vardi, Van Mooy et al. 2009; Bidle and Vardi 2011).

Furthermore, EhV86 is an icosahedral virus enveloped with a lipid membrane composed various GSLs (Vardi, Van Mooy et al. 2009) and a majority (23 of 28) of proteins comprising the mature virion possess transmembrane domains and, thus, are putative membrane proteins (Allen, Howard et al. 2008). Lipids and lipid-associated proteins appear to play a critical role in EhVs and their infection strategy, which has been shown to employ an animal-like, envelope fusion mechanism to enter and exit infected host cells(Mackinder, Worthy et al. 2009). To date, nothing is known about lipid raft characteristics in any unicellular marine phytoplankton, much less this globally, important coccolithophore.

In this study, we investigated the potential involvement of lipid rafts in *E. huxleyi*-EhV host-virus interactions. Building off of previously published methods in higher eukaryotes (Radeva and Sharom 2004; Macdonald and Pike 2005) and utilizing a flotillin-like protein in *E.huxleyi* as a biochemical marker, we developed a protocol for the isolation of lipid rafts and associated proteins from both uninfected and infected cells and characterized their dynamics and composition through genome-enabled proteomics and lipidomics. Our results provide insight into the initial key players in viral-host interactions and provide a better mechanistic understanding of the cell surface properties that serve to regulate viral infection and an innate immune response to viral infection.

1.2 Materials and Methods

1.2.1 Bioinformatic Analysis

The completed *Emiliania huxleyi* CCMP1516 genome assembly (http://genome.jgi-psf.org/Emihu1/Emihu1.home.html; v1.0) was used to search, identify,

and characterize the *E.huxleyi* flotillin-like protein (Protein ID 363433). The EhV86 genome (accession# NC 007346) was accessed through the National Center for Biotechnology Information (http://www.ncbi.nlm.nih.gov/). The BLASTP algorithm (http://blast.ncbi.nlm.nih.gov/Blast.cgi) (Altschul, Gish et al. 1990) was used for initial protein characterizations. Subsequent protein sequence analyses used the Simple Modular Architecture Research Tool (SMART) (http://smart.embl.de/) (Shultz, Milpetz et al. 1998; Letunic, Doerks et al. 2012). Secondary and tertiary structure analyses employed Protein Homology/Analog Y Recognition Engine V2.0 (PHYRE^2) (http://www.sbg.bio.ic.ac.uk/phyre2/html/page.cgi?id=index)(Kelly and Sternberg 2009) for protein fold recognition and PyMOL molecular visualization system (http://www.pymol.org/) for modeling 3D structures.

1.2.2 Host and Virus Growth and Maintenance

Emiliania huxleyi strain CCMP 1516 (*Ehux*1516) was obtained from the Provasoli-Guillard Center for Culture for Marine Phytoplankton (CCMP) and grown in f/2-Si (minus silica) under 14:10 (L:D) cycle, 200 µmol/photons $m^{-2}s^{-1}$ at 18°C with constant aeration. Cell abundance was determined using a Coulter Multisizer II (Beckman Coulter, Fullerton, CA) or flow cytometry (details below). EhV86 was propagated using *Ehux*1516 as previously described(Bidle, Haramaty et al. 2007). Virus abundance was determined by SYBR Gold staining andanalytical flow cytometry (details below).

1.2.3 Virus Infection

Experiments were designed to harvest biomass from both uninfected, 'control' *Ehux*1516 and EhV86-infected *Ehux* 1516 at 2, 24, 48 and 72 hours post infection (hpi). Exponentially growing cultures (5 L; ~2 X 10^5 cells per ml) of *Ehux* 1516 were infected with viral strain EhV86 at a multiplicity of infection (MOI) of 2. A control culture without addition of EhV86 was performed in parallel. Cultures were grown according to the conditions mentioned above. For each time point, 1 L from each culture was harvested via vacuum filtration, snap frozen in liquid N_2 and stored at -80°C until processed. Samples were also collected for cell and viral counts for each time point and analyzed daily by analytical flow cytometry (details below).

1.2.4 Flow Cytometry Analysis

Samples from each time point were counted on Influx Mariner 209s Flow Cytometer and High Speed Cell Sorter (BD Biosciences) at the Rutgers Microbial Flow Sort Lab (http://marine.rutgers.edu/flowsort/index.html). *E. huxleyi* cells were counted using chlorophyll fluorescence (692/40 nm) after triggering with forward scatter (granularity). EhV86 abundance was determined by fixation and stainingwith SYBR Gold, as previously described (Brussaard, Marie et al. 2000). Briefly, samples (40 µl) were fixed in 1% glutaraldehyde at 4°C for 15 minutes, -80°C for 5 min, and room temperature, followed by staining in 0.5X SYBR Gold (Life Technologies, Grand Island, NY) in TE buffer [10 mMTris-Cl (pH 7.8), 1 mM EDTA)] at 80°C for 10 min in the dark. Stained samples were then counted using green fluorescence (542/27 nm) after triggering with side scatter (size).

1.2.5 Lipid Raft Isolation

Frozen pellets from 2, 24, 48 and 72 hour time points were brought to 4°C on ice and suspendedin 1 ml lysis buffer (0.5% Brij-96, 25 mM Tris-HCl pH 8.0, 140 mM NaCl pH 8.0, 1 mM PMSF), which used anon-ionic detergent (Brij-96; Sigma) to solubilize all membrane and a protease inhibitor to prevent protein degradation. Samples were placed on ice for 30 minutes followed by lysate clarification for 30 minutes via centrifugation at 4°C (4000 x g). The resulting supernatants were removed and stored at -20°C for use in OptiPrep (Sigma) density gradient centrifugation. Corresponding pellets were stored at -80°C.

Detergent resistant membrane fractions from total cell lysates were isolated using 5% - 35% discontinuous OptiPrep density gradients. The supernatant from each time point was added to OptiPrep to obtain a 45% solution and placed at the bottom of 13 ml ultra-clear centrifuge tubes (Beckman #344059). The 45% OptiPrep/sample mixture was sequentially overlayed with 35% and 5% OptiPrep solutions, respectively. A blank density gradient (with no added cell lystate to the 45% OptiPrep solution) was run in parallel. Density gradients were centrifuged using a SW40 Ti Beckman rotor at 39,000 x g, 4°C, for 16 hours (protocol adapted from (Macdonald and Pike 2005). Twelve 1 ml fractions were collected by pipette in a top down fashion. Fractions 1 – 12 from each time point were aliquoted (200 µl) and stored at -80°C for subsequent proteomic, lipidomic, western immunoblotting, polymerase chain reaction (PCR) and transmission electron microscopy (TEM) analyses.

1.2.6 Western Blot Analysis

Equal volumes of density gradient sub-samples were loaded and separated on SDS-PAGE gels (Criterion TGX 4 – 20%gels; BioRad, Hercules, CA) and eletrophoretically transferred to PVDF membranes in transfer buffer (200 ml methanol, 3.03 g tris, 14.4 g glycine per 1 L of MilliQ H_20) at 100 V for 1 hour on ice. Membranes were probed with an anti-human flotillin 2 monoclonal antibody (1:500; #sc-25507; Santa Cruz Biotechnology, CA, U.S.A.) followed by polyclonal goat anti-rabbit secondary antibody (1:20,000; #sc-2004; Santa Cruz Biotechnology) and horseradish peroxidase chemiluminescence detection (SuperSignal; Pierce, Rockford, IL) using ChemiDoc MP System imager and Image Lab Software version 4.0.1 (BioRad Laboratories). Protein Plus (BioRad #161-0374) was used as a protein molecular weight standard. Human A-275 whole cell lysate of malignant melanoma cells (#sc-3811; Santa Cruz Biotechnology) was used as a positive control.

1.2.7 Transmission Electron Microscopy

TEM was used to visualize the presence and size of detergent resistant membrane vesicles. Fractions were dialysed against 200 mM Hepes buffer (pH 7.5). Dialysis of each fraction (200 µl) was achieved using a Pierce Slide-A-Lyzer 10K (10,000 mwco) dialysis cassette with 0.1 – 0.5 ml sample volume (Thermo Scientific, Rockford, IL) following manufacturer's protocol. Samples were prepared for TEM using an adapted negative staining method. Formvar/carbon-coated mesh grids (Electron Microscopy Sciences, Hatfield, PA) were subjected to ultraviolet light to remove static interference enhancing sample binding then placed on top of the dialyzed sample for 1 minute. Excess sample was wicked off using Whatman paper and then placed sample side down

onto 1% uranyl acetate solution for 1 minute. Excess stain was wicked off and grids were allowed to air dry 5 – 10 minutes before visualization. Samples were visualized at the Rutgers Electron Imaging Facility (http://cbn.rutgers.edu/emlab/emlab.html) using a JEOL 100 CX Electron microscope operating at 80kV. Digitized images were viewed and captured using a Gatan CCD 673-0200 camera connected to two high-resolution video monitors.

1.2.8 Proteomic Analysis

Frozen lipid raft fractions were sent to the Biological Mass Spectrometry Facility co-run by the UMDNJ-Robert Wood Johnson Medical School and Rutgers' Center for Advanced Biotechnology and Medicine (http://www3.cabm.rutgers.edu/home.php) for proteomic analysis via LC-MS/MS. Proteins were concentrated by vacuum aspiration (200 µl samples were reduced to 20 µl) and run ~1cm into a Novex gel Bis-Tris 10% gel. The entire gel band was excised and proteins therein were reduced, carboxymethylated, and digested with trypsin using standard facility protocols. Peptides were extracted, solubilized in 0.1% trifluoroacetic acid, and analyzed by nanoLC-MS/MS using a RSLC system (Dionex, Sunnyvale CA) interfaced with a Velos-LTQ-Orbitrap (ThermoFisher, San Jose, CA). Samples were loaded onto a self-packed 100um x 2cm trap packed with Magic C18AQ, 5um 200 A (MichromBioresources Inc, Aubum, CA) and washed with 'Buffer A' (0.2% formic acid) for 5 min with flow rate of 10 µl min^{-1}. The trap was brought in-line with the homemade analytical column (Magic C18AQ, 3um 200 A, 75 µmx50cm) and peptides fractionated at 300 n L min^{-1} using multi-step gradients of 'Buffer B' (0.16% formic acid 80% acetonitrile) consisting of 4 to 25% over 60 min and 25-55% over 30 min). Mass spectrometry data was acquired using a data-dependent

acquisition procedure with a cyclic series of a full scan acquired in Orbitrap with resolution of 60,000 followed by MSMS scans (acquired in linear ion trap) of 20 most intense ions with a repeat count of two and the dynamic exclusion duration of 60 sec.

The LC-MS/MS data was searched against the complete annotated *Emiliania huxleyi* (filtered best models; http://genome.jgi-psf.org/) and *Emiliania huxleyi* virus 86 protein databases, with the latter being parsed from Uniprot database and CRAP.fasta (www.theGPM.org). Analyses used a local version of the Global Proteome Machine (GPM cyclone, Beavis Informatics Ltd, Winnipeg, Canada) with carbamidoethyl on cysteine as fixed modification and oxidation of methionine and tryptophan as variable modifications using a 10 ppm precursor ion tolerance and a 0.4 Da fragment ion tolerance.

1.2.9 Lipidomic Analysis

Subsamples (100 µl) from OptiPrep gradient fractions were analyzed in the laboratory of Dr. Ben Van Mooy at the Woods Hole Oceanographic Institution (Woods Hole, MA) for intact polar lipids using a Thermo Scientific Triple Stage Quadrapole (TSQ) Vantage mass spectrometer. Lipids were extracted using a modified Bligh–Dyer method, as previously described (Bligh and Dyer 1959; Van Mooy and Fredricks 2010) with the phosphate buffer volume decreased by 100 µl to account for the sample. Cellular polar membrane lipids were separated by high performance liquid chromatography (HPLC) as described (Sturt, Summons et al. 2004)using an Agilent 1200 HPLC. Brij96 and OptiPrep reagents at high concentrations interfere with IPL detection by mass spectrometry, necessitating detection and quantitation by characteristic MS to MS2 neutral losses detected by triple stage quadrupole mass spectrometry

(Popendorf, Lomas et al. 2011). An authentic glucocerebrosides standard (soy, 98%, AvantiPolar Lipids) was used for initial identification of retention times and to determine tuning parameters for hGSL and vGSL detection with neutral losses of 180 Da and 162 Da, respectively. The standard was also used to calculate response factors for quantifying hGSL and vGSL. A subset of the samples were analyzed using identical high performance liquid chromatography/electrospray ionization mass spectrometry (HPLC/ESI-MS) conditions on a Thermo FTQ high-resolution Fourier-transform ion cyclotron resonance mass spectrometer (FT-ICR MS) for confirmation of elemental formulas in glycosphingolipid molecular ions and MS2 fragment ions.

Chlorophyll *a* was detected as an early eluting peak at the beginning of the intact polar lipid normal phase chromatographic method. It was identified by its characteristic photodiode array UV-visible spectrum with absorbance maxima at 431 nm (Soret Band) and 665 nm (Qy band), as well as smaller peaks at 617, 580, and 535 nm. We did not detect Pheophytin a or any other Type I chlorophyll degradation products and assume that any degradation from storage in dichloromethane or low pigment yields due to inefficient extraction by the Bligh and Dyer method is proportional in all samples. We present relative quantitation based on chromatographic peak area integration at 665 nm. UV-visible light spectra showed that there were no interfering compounds absorbing in the Qy band. The peak areas were normalized to our internal recovery standard, DNP-PE, which elutes later and has an absorbance maximum at 340 nm.

1.2.10 PCR Amplification

Polymerase chain reaction was used to amplify the EhV major capsid protein using previously published primer sequences [(Schroeder, Oke et al. 2003); EhV-MCP-

F1, 5'-GTC TTC GTA CCA GAA GCA CTC GCT-3'; EhV-MCP-R1 5'-ACG CCT CGG TGT ACG CAC CCT CA-3']. PCR reaction conditions were as follows: 5 µl of each fraction was directly added to a 15 µl reaction cocktail mixture containing 1 U *RedTaq* DNA polymerase (Promega), 1 x PCR reaction buffer (Promega), 0.25 mMdNTPs, and 30 pmol of each primer. PCR reactions were run in a Master cycler epgradient S (Eppendorf, NY, U.S.A.) with an initial high temperature cycle to lyse intact viral capsids (8°C, 65°C, 97°C x 3 cycles) followed by an initial denaturing step of 94°C (5 min), and 30 cycles of denaturation at 94°C (30 s), annealing at 55°C (30 s), and extension at 72°C (45 s). PCR amplicons were run on a 1% agarose gel (w/v) in 1 x TAE at 80 V for 1.5 hours, stained with ethidium bromide (0.5 µg ml^{-1}) and visualized using ChemiDoc MP System imager and Image Lab Software version 4.0.1 (BioRad Laboratories). EZ Load 100 bp molecular weight marker (BioRad; Cat #170-8352) was used as a DNA sizing standard. Purified genomic DNA *Ehux* strain CCMP 373 and fresh EhV86 viral lysate served as negative and positive template controls, respectively.

1.3 Results and Discussion

The important functional roles of lipid membranes, glycosphingolipids (GSLs), and PCD activation (via ROS, metacaspase expression, and caspase activity) in viral infection of *E. huxleyi*(Bidle, Haramaty et al. 2007; Mackinder, Worthy et al. 2009; Vardi, Van Mooy et al. 2009) raise fundamental questions about controls on their *de novo* synthesis, composition, and activation in the context of host physiological response and sensitivity. Given their enrichment in GSLs and involvement in sensing extracellular stimuli and activating signaling cascades through protein-protein interactions (Simons

and Toomre 2000), lipid rafts likely play a fundamental role in *E.huxleyi*-EhV host-virus interactions, viral infectivity, and host resistance mechanisms. To date, lipid rafts, and their associated protein and lipid compositions, have not been characterized in any unicellular algae, much less *E. huxleyi*. A primary goal of this study was to isolate and characterize lipid rafts, here defined as detergent insoluble membranes (DRMs), especially their associated proteomes and lipidomes, in both uninfected and EhV86-infected cells. Our approach was to use flotillin and GSL species as respective protein and lipid biochemical markers to inform our targeted isolation of lipid rafts for more detailed characterization.

Flotillins are expressed in a wide variety of eukaryotes and prokaryotes and play a central role in lipid raft generation (protein- lipid binding domain), as well as in the stabilization of raft-associated proteins (protein-protein binding domain), both of which are fundamental in the regulation of diverse processes (i.e. signal transduction, membrane trafficking and pathogen entry) (Borner, Sherrier et al. 2005; Morrow and Parton 2005). Bioinformatic analysis of the *Emiliania huxleyi* CCMP 1516 annotated proteome revealed a 306 amino acid, 33.5 kDaflotillin-like protein (Protein ID 363433), which contained the evolutionary conserved Prohibitin Homology (PHB)/StomatinProhibitinFlotillin Homology (SPFH) domain at residues 4 – 166 using predicted secondary structure analysis (Fig. 1.1 A). Within this conserved domain lies two hydrophobic Sphingolipid Binding Domains (SBDs; amino acid residues 13 – 41 and 133 - 151) along with a conserved palmitoylation site, both of which contribute to membrane association (Morrow, Rea et al. 2002; Morrow and Parton 2005). The required post-translational palmitoylation of flotillins at the N-terminus follows their

synthesis on ribosomes and an unusual golgi-independent trafficking pathway targets the protein to the plasma membrane (Morrow, Rea et al. 2002). The C-terminal end of the *E. huxleyi* flotillin-like protein has a predicted α-helix coil at residues 266 – 286 (Fig. 1.1 A), which is characteristic of all classic flotillins and thought to oligomerize with other flotillin molecules (Morrow and Parton 2005; Solis, Hoegg et al. 2007). The presence of three adjacent α-helix coils within this domain allow for the oligomerization of flotillin in higher eukaryotes (Solis, Hoegg et al. 2007). Exposed lysine residues are thought to facilitate a high-affinity, stable covalent linkage between flotillin monomers (Solis, Hoegg et al. 2007). Modeling of the tertiary structureof the *E. huxleyi* flotillin-like protein using Phyre2 software and PyMOL software (Fig. 1.1 B) successfully visualized this dimerizing α-helix coil tail (Fig. 1.1 B). Western immunoblot analysis with a monoclonal antibody raised against human flotillin-2 (NCBI Accession#Q14254) detected the expression of a prominent 67 kDa band in *E. huxleyi* 1516, consistent with the predicted dimer of the flotillin-like protein (Fig. 1.1 C). Immunoblot analysis also successfully detected the predicted 47 kDa human flotillin in human A-375 whole cell lysate of malignant melanoma cells, thereby serving as a positive control for our analysis.

Lipid raft dynamics, isolation, and characterization

We investigated lipid raft dynamics and composition both in control host cells (uninfected) and during host-viral interactions at 2, 24, 48, and 72 hours post infection (hpi) to not only determine the lipid raft landscape in healthy cells, but to also determine if and how lipid rafts are altered by viral infection. We first confirmed successful lytic infection of *E. huxleyi* 1516 with EhV86 (moi=2), which resulted in a notable reduction

of host cell abundance over 72 hours (h) compared to uninfected control cells (Fig. 1.2 A); infected cells only reached host cell abundances of ~1.25 x 10^6 cells ml^{-1}at 72 h, while uninfected cell abundance climed to 2.5 x 10^6 cells ml^{-1}. Uninfected *E. huxleyi* cells continued to increase in abundance over the time course of the experiment. EhV86 abundance increased by over two orders of magnitude between 24 and 72 hours post infection (Fig. 1.2 B), concomitant with decreases in host growth rates (Fig. 1.2 A).

We developed a purification method, based on published techniques to isolate lipid rafts from higher eukaryotes, employing lysis and homogenization of cells in a non-ionic detergent (Brij-96) followed by ultracentrifugation in a discontinuous (5 – 35%) OptiPrep density gradient (Fig. 1.3 A-B). Detergent resistant lipid rafts from higher eukaryotic cells have been isolated using the detergent Triton X-100 followed by sucrose gradient fractionation, whereby fractions enriched in sphingolipids, cholesterol, and raft marker proteins flotillin and GPI-linked proteins distribute in the top few, less dense fractions (Munro 2003; Pike 2003; Radeva and Sharom 2004; Macdonald and Pike 2005). Radeva and Sharom (2004) have also investigated lipid raft molecular properties after isolation using two different non-ionic detergents, Triton X-100 and Brij-96. Interestingly, it was reported that DRM vesicle orientation, as well as their protein composition, differed depending on the detergent used, with Brij-96 forming 'outside-in' oriented vesicles with lower density (fractions 2 – 4) and Triton X-100 yielding 'inside-out' vesicles of higher density (fractions 5 – 7). DRM vesicle size (~200 nm) was comparable for the two detergents (Pike 2003; Radeva and Sharom 2004). In this study, Brij-96 was used in order to produce 'outside-in' DRMs and subsequently identify and characterize lipid raft-associated proteins found on the extracellular plasma membrane of

E. huxleyi uninfected and EhV86-infected cells. Direct visualization of lipid vesicles in select fractions via transmission electron microscopy showed the presence of prominent, 0.2 μm DRM vesicles in Fractions 2 and 3 only for both uninfected controls and EhV86-infected samples (Fig. 1.3 C). This is consistent with published characteristics of DRMs in higher eukaryotes (Pike 2003; Radeva and Sharom 2004). No lipid vesicles were seen in higher density fractions for either treatment.

PCR amplification of the EhV86 major capsid protein (MCP) was used as a proxy to identify the distribution of EhVs (and associated DNA) in OptiPrep density gradient fractions from EhV86-infected cells at 2, 24, 48 and 72 hpi (Fig. 1.4). This helped provide an initial characterization of the OptiPrep density fractions and important context on where to expect viruses (and their associated vGSLs and proteins). Successful amplification of the expected 248 bp MCP amplicon was observed for all samples confirming the presence of EhV genomic DNA. Prominent MCP amplicons were only detected in fractions 6 – 12 for both 2 and 24 h post infection, indicating the selective presence of virus in higher density fractions (Fig. 1.4). The dramatic increase in EhV abundance (10- to 100-fold) during late lytic phase (48 – 72 h) was clearly reflected in the increased intensity MCP amplification in fractions 6 – 12. However, notable, but much weaker, amplification of EhV MCP was also seen in lower density fractions (1 – 5) at these time points. Our MCP amplicon data could represent the distribution of intact EhV virions or the released EhV genomic DNA within the OptiPrep fractions. We also tried to locate and quantify EhV abundance in OptiPrep fractions via SYBR-Green staining and flow cytometry, but were unable to see a recognizable EhV population signal, compared to a fresh EhV86 stock culture (data not shown). Brij-96 treatment of a

fresh EhV86 stock sample was found to compromise the SYBR-Green population signal on flow cytometry, so we deduce that our MCP amplicon data reflects the distribution of released EhV86 genomic DNA. Our data is consistent with EhVs having a membrane enveloped structure (Mackinder, Worthy et al. 2009) that is disrupted by non-ionic detergent treatment.

Anti-flotillin immunoblot analysis was performed on 2 and 48 h control and EhV86-infected *E. huxleyi* fractions to identify flotillin-containing fractions. Strong immunohybridization was observed to a prominent 67 kDa flotillin-like protein (Fig. 1.1 C) in both *E. huxleyi* control and EhV86-infected fractions at both time points. Uninfected *E. huxleyi* fractions showed strong immunohybridization of the 67 kDa flotillin-like protein among the low density fractions 1 – 5 (Fig. 1.5, upper panels). The pattern of anti-flotillin immunohybridization was dramatically different in EhV86-infected cells, instead being characterized by a more defined and focused signal in fractions 2 and 3 at 2 and 48 hpi, respectively (Fig. 1.5, lower panels). These results clearly demonstrate that interaction of *E. huxleyi* host cells with EhV86 virions, even for short time periods (2 hpi), has a pronounced affect on the physical attributes of flotillin-associated DRMs. Taken together, our physical (TEM), molecular (distribution of MCP-amplicons), and biochemical (anti-flotillin western immunoblot analysis) results highlighted fraction 2 as a strong candidate for subsequent characterization of the lipidome and proteome associated with isolated lipid rafts.

Distribution and composition of glycosphingolipids

Glycosphingolipids are polar lipids that critically 'lubricate' *E. huxleyi*-EhV interactions both in culture (Vardi, Van Mooy et al. 2009; Bidle and Vardi 2011) and in natural systems (Vardi, Haramaty et al. 2012). Indeed, host-specific glycosphingolipids (hGSLs), consisting of palmitoyl-based glycosphingolipids (Vardi, Haramaty et al. 2012) and viral glycosphingolipids (vGSLs), consisting myristoyl-based glycosphingolipids (Vardi, Van Mooy et al. 2009; Vardi, Haramaty et al. 2012), play important functional roles in the infection of *E. huxleyi* and even serve to trace both host and virus populations, respectively (Vardi, Haramaty et al. 2012). Knowing GSLs classically play prominent roles in lipid rafts of higher eukaryotes, we examined their relationship to DRMs in *E. huxleyi* and determined which GSLs, if any, coincide with the flotillin biochemical protein marker of lipid rafts. Using high performance liquid chromatography/triple stage quadrapole mass spectrometry (HPLC/TSQ-MS), we examined the abundance and chemical identity of GSLs in the OptiPrep fractions from control and EhV86-infected cells at 2, 48, and 72 h. While a variety of GSL species were detected in our analysis, we grouped them into three general classes: 'hGSL', host-specific GSLs based on the d19:3 long chain base and either a C22:3 hydroxy- or C22:2 hydroxy-fatty acid (Vardi, Haramaty et al. 2012); 'hGSL-b's, short chain (C15 – C19) monounsaturated fatty acids that did not increase with EhV infection (thereby also host-specific); and 'vGSLs', myristoyl-based GSLs with C15 – C24 saturated fatty acids and C20 – C24 monounsaturated fatty acids (Vardi, Van Mooy et al. 2009).

Total GSL production (normalized to the glucocerebroside recovery standard, DNP-PE) was generally confined to higher density, lower fractions (6 – 12; Fig. 1.5),

indicating that most GSLs were not associated with DRMs. Among the different classes of GSLs, hGSLs were generally confined to the lower fractions (5 – 12) and comprised a relatively high percentage of GSLs in uninfected control cells within each fraction (30 – 98%). The other class of host-specific GSLs, hGSL-b, showed a very different distribution in the OptiPrep density gradients (Fig. 1.5, Table 1.1); instead being concentrated in the upper, low density fractions (1 – 3) and accounting for up to 94% of GSLs in these fractions. These host GSLs clearly behaved differently in the density gradients, with the hGSL-b class closely corresponding to other lipid raft physical (presence of DRMs, Fig. 1.3) and biochemical markers (distribution of flotillin, Fig. 1.4) and thereby more likely representing the lipid-raft lipidome. Interestingly, we did detect prominent chemical signatures so called 'vGSLs' in uninfected control cells at all time points suggesting that this class of GSLs, as defined above (Table 1.1), contain a diverse set of chemical species also characteristic of the host lipidome. Clearly, these particular vGSL species do not derive from EhVs, given they were detected in an uninfected host. We attribute this to the fact that the host and virus share core GSL biosynthetic machinery through lateral gene transfer(Monier, Pagarete et al. 2009), so it is not surprising that they share similar myristoyl-based GSL species. Nonetheless, their distribution largely paralleled the hGSL-b type and, therefore, is also implicated in lipid raft composition.

Viral infection triggered a massive up-regulation (3 – 10-fold) in the normalized total GSL production at 48 h and especially 72 h post infection, with most GSLs being confined to fractions 6 – 12 (Fig. 1.5). The hGSL distribution and percent contribution at 2 h was notably similar between control and infected cells. Infection with EhV86

subsequently down-regulated hGSL production at 48h and even more so at 72 h, where by hGSLs comprised only 14 – 26% of GSLs in fractions 5 – 12. For comparison, hGSLs accounted for 68 – 98% of GSLs for uninfected control fractions. Likewise, virus infection significantly down-regulated the relative production of hGSL-b species, especially at 72 h post infection, where these lipids were almost completely removed from much of the fractionated lipidome. In contrast, vGSLs dominated the GSL composition over the course of infection, and were generally distributed throughout all 12 fractions at 48 and 72 h. At 72 h post-infection vGSLs accounted for an impressive 73 – 97% of GSLs in all fractions. This distribution of vGSLs corresponded quite well with our PCR-based amplification of the EhV MCP gene, indicating that genomic DNA and viral membranes (which consist largely of vGSLs) co-localized in our density gradients.

Characterizing the lipid raft proteome

We targeted fraction 2 from both control and EhV86-infected samples at 2 hpi for proteomic analyses in order to provide insight into the key protein players in initial viral-host interactions and provide a better understanding of the cell surface proteins that serve to regulate viral infection and an innate immune response. The LC-MS/MS peptide fragment data was searched against the respective *E. huxleyi* 1516 and EhV86 annotated proteome databases with amino acid sequences parsed from Uniprot database and CRAP.fasta. A total of 86 proteins were identified in the control *E. huxleyi* 1516 sample where as 116 total proteins were found in the EhV86-infected sample. An analysis of the top 20 protein hits (protein log-e rank order) for both control and EhV86-infected samples (Tables 1.3 and 1.4), first identified an *E. huxleyi* Band_7, flotillin-like protein

(Protein ID 363433; log e= -109.1; 34 unique peptides) with the predicted SPFH-containing domain, corroborating our anti-flotillin Western blot analyses and further supporting fraction 2 as a bonafide lipid raft fraction. Our proteomic analysis also identified several known membrane proteins; including an outer membrane porin, nitrate/nitrate transporters, an import receptor, a sodium/calcium exchange membrane protein, and a substrate carrier protein. Carrier proteins are integral membrane proteins that are involved in the movement of ions, small molecules or macromolecules, such as another protein, across biological membranes. These all provided confidence in the membrane-containing nature of our lipid-raft proteome. Interestingly, we also detected a variety of chlorophyll a/b binding proteins among our top 20 protein hits. Together with our observations that the chlorophyll pigment distribution in Optiprep density gradients did not coincide with our lipid raft fractions and instead was maximal in lower more dense fractions (Figure 1.7), these findings suggest that lipid rafts (and associated proteins) exist in thylakoid membranes and are features of subcellular organelles, not surprising given the roles that lipid rafts play in normal cell trafficking.

We were particularly interested in the pool of stress-, PCD-, and/or innate immunity-related proteins associated with lipid rafts given the clear interface of EhV infection with host stress and PCD pathways (Bidle, Haramaty et al. 2007; Vardi, Van Mooy et al. 2009; Bidle and Vardi 2011; Bidle and Kwityn 2012). At the same time, we wanted to investigate whether unique proteins (of both known and unknown function) characterized respective uninfected (Tables1.5 – 1.6) and EhV86-infected (Tables 1.7 – 1.8) cell states, in order to better differentiate the 'basal' host lipid-raft proteome from a virus-manipulated one. Our analysis revealed that *E. huxleyi* cells not only have a basal lipid

raft proteome composition, but EhVs clearly alter this composition during early infection processes.

The 'basal' lipid raft proteome (Table 1.5) of healthy *E. huxleyi* cells encompassed a wide range of proteins, whose homologues and evolutionary conserved domains are widespread in higher eukaryotes and are involved in the regulation of normal cell function. These included Beta-gamma crystallin (440685), fibronectin (205013), ferredoxin (109218), tetratricopeptide repeat (TPR) proteins (212473), ankyrins (448295, 450475, 450932), a HEAT repeat protein (115688), and a WD40-containing Sec31-like secretory protein (460451), which are integral proteins to specialized membrane domains within the plasma membrane that act as transporters, scaffolds or adaptors and mediate protein-protein interactions, intracellular trafficking, or vesicle transport (Mohler, Gramolini et al. 2002; Cortajarena and Regan 2006; Suman, Mishra et al. 2011). Several notable stress and defense proteins were also identified as unique to healthy *E. huxleyi* lipid rafts, such as phagocyte-NADPH-oxidase (Phox) –like (450438), ubiquitin-ligase activity related (Ubox) (203844), and patatin(468714) proteins. Phox-like proteins possess an ability to generate superoxide (Kawahara and Lambeth 2007) and play an important role in host defense, participating in a microbicidal complex. U-box domain proteins, most commonly found in plants,are thought to act as negative regulators in cell death signaling (Zeng, Park et al. 2008). Also found in plants, participating in defense as well as signal transduction, are the patatin proteins, a group of glycoproteins showing lipolytic activity sharing a conserved domain with human phospholipase A2 (Banerji and Flieger 2004).

A total of 34 proteins were found to be unique to the EhV86 viral infected cell state at 2 hpi (Table 1.7), with a majority having putative involvement in lipid trafficking, signal transduction processes, and innate immune response. CRAL/TRIO domain-containing proteins (449182) regulate intracellular trafficking of hydrophobic ligands by binding small lipophilic molecules (Panagabko, Morley et al. 2003). The DENN/MADD (differentially expressed in normal and neoplastic cells/MAPK-activating protein containing a death domain; 459348) domain containing proteins are known adaptors linking type 1 tumor necrosis factor receptor (TNFR1) to the induction of MAP kinases, known mediators of stress-induced apoptosis, as well as regulators of RabGTPases, recruiting effectors that control membrane trafficking (Schievella, Chen et al. 1997; Marat, Dokainish et al. 2011). Proline-rich extensins (PRICHEXTENSN; 443600), plant membrane-spanning proteins, play a role in pathogen defense as an early warning system, activating downstream defense mechanisms through signal transduction due to a compromised cell wall (Silva and Goring 2002; Sanabria, Huang et al. 2010). The WD40-containing U5 snRNP-specific protein (53698) combine with unmodified pre-mRNA and various other proteins to form a spliceosome (Lerner, Boyle et al. 1980) a large RNA-protein molecular complex upon which splicing of pre-mRNA occurs and a critical aspect of post-transcriptional modification of RNA. WD40 motifs act as sites for protein-protein interaction and protein assembly platforms, involved in cell cycle control, signal transduction and apoptosis (Xu and Min 2011). Likewise, PHD-type zinc finger domains (373476) are also thought be involved in protein-protein interaction and be important for the assembly or activity of multicomponent complexes involved in transcriptional activation or repression (Aasland, Gibson et al. 1995). Basic cysteine-rich

peptides containing a hairpin loop domain (212522), defensins, are part of a larger family of antimicrobial peptides (AMPs) produced by the innate immune system to combat invading pathogens (Broekaert, Terras et al. 1995). Of significance is the presence of toll interleukin 1 receptor (TIR; 466323) and leucine rich repeat (LRR; 114838) domain proteins, connected through a nucleotide binding (NB) domain, mediate pathogen recognition and activate host-cell defense responses (Inohara, Chamaillard et al. 2005; Peart, Mestre et al. 2005; Swiderski, Birker et al. 2009). TIR-NB-LRR proteins have been shown to recognize viral membrane proteins through ligand-receptor interaction resulting in the plant hypersensitive response (HR), a form of stress-induced PCD (Heath 2000; Nimchuk, Eulgem et al. 2003).

The classic ligand-binding partner for toll-like receptors (TLR/TIR) are C-type lectin-containing proteins (Neilan, Borca et al. 1999). C-type lectin-containing proteins, involved in cell-cell adhesion and endocytosis, have been reported in poxviruses and African swine fever virus (ASFV) mediating the early events involving host cell attachment and subsequent internalization (Neilan, Borca et al. 1999; Cambi, Koopman et al. 2005). Here, we detected the presence of an EhV86 C-type lectin 1 domain–containing membrane protein (ehv149; Q4A2Y5), in the virally infected *E. huxleyi* lipid raft fraction at 2 hpi, which directly implicates lipid raft domains as viral entry and/or exit sites. This protein was among the 23 putative membrane proteins (with transmembrane domains) detected in the mature EhV virion proteome (Allen, Howard et al. 2008). Microarray analysis has classified expression of ehv149 transcripts to within 2 hpi window, so it is unclear if our proteomic analysis represents entry or exit of EhVs. Nonetheless, it implicates a possible protein-protein (TIR-NB-LRR/C-type Lectin)

specific binding interaction between *E. huxleyi* 1516 and EhV86 for the successful attachment to host cell membranes for viral entry or exit through lipid rafts (Neilan, Borca et al. 1999; Nimchuk, Eulgem et al. 2003; Cambi, Koopman et al. 2005; Swiderski, Birker et al. 2009). Notably, the other C-type lectin 2 domain-containing protein (ehV060) in the mature EhV proteome (Allen, Howard et al. 2008) was not detected in our lipid raft proteome analysis so it is unclear whether it also interacts with lipid rafts. A truncated version of this particular protein (ehv060) resides in ehv163 (Allen, Schroeder et al. 2006), another *Coccolithovirus* that, unlike EhV86, is unable to infect *Ehux* 1516. In light of our lipid raft proteome data, it is tempting to speculate that the interactions of these C-type lectin-containing proteins with lipid raft proteins are key conduits to successful infection and targets of cellular resistance mechanisms.

Conclusion

Lipid rafts exist as small microdomains (~50 nm) containing a small subset of raft-associated proteins (Simons and Ehehalt 2002; Morrow and Parton 2005). Due to raft coalescence, these raft domains not only increase in size but can lead to novel protein composition triggering specific cellular processes. Instigation of lipid raft domain clusters can be activated extracellularly through ligands, lectins, or antibodies, oligomerization of proteins within the plasma membrane bilayer, or through adaptors and scaffolding proteins found on the cytosolic surface of the membrane (Simons and Toomre 2000; Simons and Ehehalt 2002) resulting in the exclusion of or increased affinity for given proteins. Downstream cellular processes such as signal transduction and PCD pathways due to host-virus interactions of *E. huxleyi* and EhV86 have been described

(Bidle 2007; Vardi, Van Mooy et al. 2009; Bidle and Vardi 2011; Vardi, Haramaty et al. 2012), but, to date, key players involved in initial *E. huxleyi* resistance and defense and EhV86-specific host attachment and entry sites have remained elusive.

In this study, we have demonstrated the successful isolation of lipid rafts using host glycosphingolipids and flotillin as lipid and protein biomarkers, respectively, in order to characterize raft-associated proteins involved in host-virus interactions. Our data show that viral infection plays a significant role in the rapid change in lipid and protein composition of lipid rafts. Our analyses provide the first direct evidence of an innate immune system in *Emiliania huxleyi* 1516, which are induced by EhV86 entry and/or exit and possibly through the binding to lipid raft specific proteins. Further research on the functionality of raft-associated proteins and their response to viral infectivity will elucidate cross-talk pathways between these proteins and those triggering downstream pathways such as PCD. Proteomic analyses of 24 h post infection fraction 2 will allow further insight into raft-associated proteins that facilitate viral exit strategies. Moreover, the application of methods used in this study to various sensitive and resistant strains of *E. huxleyi* to EhV86 infection will further implicate raft-associated proteins role in host-viral interactions and as critical determinants of infectivity.

References

Aasland, R., T. Gibson, et al. (1995). "The PHD finger: implications for chromatin-mediated transcriptional regulation." Trends in Biochemistry Science **20**: 56 - 59.

Allen, M. J., J. A. Howard, et al. (2008). "Proteomic analysis of the EhV-86 virion." Proteome Science **6**(11).

Allen, M. J., D. C. Schroeder, et al. (2006). "Genome comparison of two Coccolithoviruses." Virology Journal **3**: 15.

Allen, M. J., D. C. Schroeder, et al. (2006). "Evolutionary History of the Coccolithoviridae." Molecular Biology and Evolution **23**(1): 86 - 92.

Altschul, S. F., W. Gish, et al. (1990). "Basic local alignment search tool." Journal of Molecular Biology **215**: 403 - 410.

Babuke, T. and R. Tikkanen (2007). "Dissecting the molecular function of reggie/flotillin proteins." European Journal of Cell Biology **86**: 525 -532.

Banerji, S. and A. Flieger (2004). "Patatin-like proteins: a new family of lipolytic enzymes present in bacteria?" Microbiology **150**(3): 522 - 525.

Bidle, K. D., L. Haramaty, et al. (2007). "Viral activation and recruitment of metacaspases in the unicellular coccolithophore, Emiliania huxleyi." PNAS **104**(14): 6049 - 6054.

Bidle, K. D. and C. J. Kwityn (2012). "Assessing the role of caspase activity and metacaspase expression on viral susceptibility of the coccolithophore, Emiliania huxleyi (Haptophyta)." Journal of Phycology **48**(5): 1079 - 1089.

Bidle, K. D. and A. Vardi (2011). "A chemical arms race at sea mediates algal host-virus interactions." Current Opinion in Microbiology **14**: 1 - 9.

Bidle, K. D. H., Liti; Barcelos e Ramos, Joana; Falkowski, Paul (2007). "Viral activation and recruitment of metacaspases in the unicellular coccolithophore, Emiliana huxleyi." PNAS **104**(14): 6049-6054.

Bligh, E. G. and W. J. Dyer (1959). "A rapid method of total lipid extraction and purification." Canadian Journal of Physiology and Pharmacology **37**: 911 - 917.

Borner, G. H., D. J. Sherrier, et al. (2005). "Analysis of Detergent-Resistant Membranes in Arabidopsis. Evidence for Plasma Membrane Lipid Rafts." Plant Physiology **137**: 104 - 116.

Bratbak, G., J. K. Egge, et al. (1993). "Viral mortality of the marine alga Emiliania huxleyi (Haptophyceae) and termination of algal blooms." Marine Ecology Progress Series **93**(39 - 48).

Broekaert, W. F., F. R. Terras, et al. (1995). "Plant defensins: novel antimicrobial peptides as components of the host defense system." Plant Physiology **108**: 1353 - 1358.

Brown, D. A. and E. London (2000). "Structure and Function of Sphingolipid- and Cholesterol-rich Membrane Rafts." The Journal of Biological Chemistry **275**.

Brussaard, C. P. D., D. Marie, et al. (2000). "Flow cytometric detection of viruses." Journal of Virological Methods **85**: 175-182.

Cambi, A., M. Koopman, et al. (2005). "How C-type lectins detect pathogens." Cellular Microbiology **7**(4): 481 - 488.

Castberg, T., R. Thyrhaug, et al. (2002). "Isolation and characterization of a virus that infects Emiliania huxleyi (Haptophyta)." Journal of Phycology **38**(4): 767 - 774.

Cortajarena, A. L. and L. Regan (2006). "Ligand binding by TPR domains." Protein Science **15**(5): 1193 - 1198.

Dassow, P. v., H. Ogata, et al. (2009). "Transcriptome analysis of functional differentiation between haploid and diploid cells of Emiliania huxleyi, a globally significant photosynthetic calcifying cell." Genome **10**(10): R114.

del Cacho, E., M. Gallego, et al. (2007). "Expression of Flotillin-1 on Eimeria Tenella Sporozoites and its Role in Host Cell Invasion." Journal of Parasitology **93**(2): 328 - 332.

Edidin, M. (2003). "The State of Lipid Rafts: From Model Membranes to Cells." Annual Review of Biophysics and Biomolecular Structure **32**: 257-283.

Hakomori, S.-i. (2008). "Structure and function of glycosphingolipids and sphingolipids: Recollections and future trends." Biochimica et Biophysica Acta **1780**: 325 - 346.

Hancock, J. F. (2006). "Lipid rafts: contentious only from simplistic standpoints." Nature **7**.

Heath, M. C. (2000). "Hypersensitive response-related death." Plant Molecular Biology **44**: 321 - 334.

Inohara, N., M. Chamaillard, et al. (2005). "NOD-LRR Proteins: Role in Host-Microbial Interactions and Inflammatory Disease." Annual Review of Biochemistry **74**: 355 - 383.

Jordan, R. W. and A. H. L. Chamberlain (1997). "Biodiversity among haptophyte algae." Biodiversity and Conservation **6**: 131 - 152.

Kawahara, T. and J. D. Lambeth (2007). "Molecular evolution of Phox-related regulatory subunits for NADPH oxidase enzymes." BMC Evolutionary Biology **7**.

Kelly, L. A. and M. J. E. Sternberg (2009). "Protein structure prediction on the web: a case study using the Phyre server." Nature Protocols **4**: 363 - 371.

Langhorst, M. F., A. Reuter, et al. (2005). "Scaffolding microdomains and beyond: the function of reggie/flotillin proteins." Cellular and Molecular Life Sciences **62**: 2228 - 2240.

Lerner, M., J. Boyle, et al. (1980). "Are snRNPs involved in splicing?" Nature **283**: 220 - 224.

Letunic, I., T. Doerks, et al. (2012). "SMART 7: recent updates to the protein domain annotation resource." Nucleic Acids Research **40**(D1): D302 - D305.

Lingwood, D. and K. Simons (2010). "Lipid Rafts As a Membrane-Organizing Principle." Science **327**: 46 - 50.

Macdonald, J. L. and L. J. Pike (2005). "A Simplified Method for the Preparation of Detergent-free Lipid Rafts." Journal of Lipid Research **46**(5): 1061-1067.

Mackinder, L. C., C. A. Worthy, et al. (2009). "A unicellular algal virus, Emiliania huxleyi virus 86, exploits an animal-like infection strategy." Journal of General Virology **90**: 2306 - 2316.

Marat, A. L., H. Dokainish, et al. (2011). "DENN Domain Proteins: Regulators of Rab GTPases." Journal of Biological Chemistry **286**(16): 13791 - 13800.

Mohler, P. J., A. D. Gramolini, et al. (2002). "Ankyrins." Journal of Cell Science **115**: 1565 - 1566.

Monier, A., A. Pagarete, et al. (2009). "Horizontal gene transfer of an entire metabolic pathway between a eukaryotic alga and its DNA virus." Genome Research **19**(8): 1441 - 1449.

Morrow, I. C. and R. G. Parton (2005). "Flotillins and the PHB Domain Protein Family: Rafts, Worms and Anaesthetics." Traffic **6**: 725 - 740.

Morrow, I. C., S. Rea, et al. (2002). "Flotillin-1/reggie-2 traffics to surface raft domains via a novel golgi-independent pathway. Identification of a novel membrane targeting domain and a role for palmitoylation." Journal of Biochemistry **277**: 48834 - 48841.

Munro, S. (2003). "Lipid Rafts: Elusive or Illusive?" Cell **115**: 377 - 388.

Neilan, J. G., M. V. Borca, et al. (1999). "An African swine fever virus ORF with similarity to C-type lectins is non-essential for growth in swine macrophages in vitro and for virus virulence in domestic swine." Journal of General Virology **80**: 2693 - 2697.

Nimchuk, Z., T. Eulgem, et al. (2003). "Recognition and Response in the Plant Immune System." Annual Review of Genetics **37**: 579 - 609.

Panagabko, C., S. Morley, et al. (2003). "Ligand Specificity in the CRAL-TRIO Protein Family." Biochemistry **42**: 6467 - 6474.

Peart, J. R., P. Mestre, et al. (2005). "NRG1, a CC-NB-LRR Protein, together with N, a TIR-NB-LRR, Mediates Resistance against Tobacco Mosaic Virus." Current Biology **15**: 968 - 973.

Pike, L. J. (2003). "Lipid rafts: bringing order to chaos." Journal of Lipid Research **44**.

Popendorf, K. J., M. W. Lomas, et al. (2011). "Microbial sources of intact polar diacylglycerolipids in the Western North Atlantic Ocean." Organic Geochemistry **42**: 803-811.

Radeva, G. and F. J. Sharom (2004). "Isolation and characterization of lipid rafts with different properties from RBL-2H3 (rat basophilic leukaemia) cells." Journal of Biochemistry **380**: 219 - 230.

Rajendran, L. and K. Simons (2005). "Lipid rafts and membrane dynamics." Journal of Cell Science **118**: 1099 - 1102.

Rivera-Milla, E., C. A. O. Struermer, et al. (2006). "Ancient origin of reggie (flotillin), reggie-like, and other lipid-raft proteins: convergent evolution of the SPFH domain." Cellular and Molecular Life Sciences **63**: 343 - 357.

Sanabria, N. M., J.-C. Huang, et al. (2010). "Self/nonself perception in plants in innate immunity and defense." Self Nonself **1**(1): 40 - 54.

Schievella, A. R., J. H. Chen, et al. (1997). "MADD, a Novel Death Domain Protein That Interacts with the Type I Tumor Necrosis Factor Receptor and Activates Mitogen-activated Protein Kinase." The Journal of Biological Chemistry **272**(18): 12069 - 12075.

Schroeder, D. C., J. Oke, et al. (2003). "Virus Succession Observed During an Emiliania huxleyi Bloom." Applied and Environmental Microbiology **69**(5): 2484 - 2490.

Schroeder, D. C., J. Oke, et al. (2002). "Coccolithovirus (Phycodnaviridae): Characterisation of a new large dsDNA algal virus that infects Emiliania huxleyi." Archives of Virology **147**: 1685 - 1698.

Shultz, J., F. Milpetz, et al. (1998). "SMART, a simple modular architecture research tool: Identification of signaling domains." PNAS **95**(11): 5857 - 5864.

Silva, N. F. and D. R. Goring (2002). "The proline-rich, extensin-like receptor kinase-1 (PERK1) gene is rapidly induced by wounding." Plant Molecular Biology **50**: 667 - 685.

Simons, K. and R. Ehehalt (2002). "Cholesterol, lipid rafts, and disease." The Journal of Clinical Investigation **110**(5).

Simons, K. and D. Toomre (2000). "Lipid Rafts and Signal Transduction." Molecular Cell Biology **1**: 31 - 41.

Solis, G. P., M. Hoegg, et al. (2007). "Reggie/flotillin proteins are organized into stable tetramers in membrane microdomains." Biochemical Society **403**: 313 - 322.

Staskawicz, B. J., M. B. Mudgett, et al. (2001). "Common and contrasting themes of plant and animal diseases." Science **292**: 2285 - 2289.

Sturt, H. F., R. E. Summons, et al. (2004). "Intact polar membrane lipids in prokaryotes and sediments deciphered by high-performance liquid chromatography/electrospray ionization multistage mass spectrometry - new biomarkers for biogeochemistry and microbial ecology." Rapid Communications in Mass Spectrometry **18**(617 - 628).

Suman, S. K., A. Mishra, et al. (2011). "Evolutionary remodelling of the Betagamma-crystallins for domain stability at the cost of Ca2+-binding." Journal of Biological Chemistry **286**: 43891 - 43901.

Swiderski, M. R., D. Birker, et al. (2009). "The TIR Domain of TIR-NB-LRR Resistance Proteins Is a Signaling Domain Involved in Cell Death Induction." The American Phytopathological Society **22**(2): 157 - 165.

Thierstein, H. R. and J. R. Young (2004). Coccolithophores From Molecular Processes to Global Impact. Germany, Springer.

van der Goot, F. G. and T. Harder (2001). "Raft membrane domains from a liquid-ordered membrane phase to a site of pathogen attack." Seminars in Immunology **13**: 89 - 97.

Van Etten, J. L. G., MV; Muller, DG; Boland, W; Delaroque, N (2002). "Phycodnaviridae -- large DNA algal viruses." Archives of Virology **147**: 1479-1516.

Van Meer, G. and K. Simons (1988). "Lipid polarity and sorting in epithelial cells." Journal of Cell Biochemistry **36**: 51-58.

Van Mooy, B. A. and H. F. Fredricks (2010). "Bacterial and eukaryotic intact polar lipids in the eastern subtropical South Pacific: water-column distribution, planktonic sources, and fatty acid composition." Geochimica Cosmochimica Acta **74**: 6499 - 6516.

Van Valen, L. (1973). "A new evolutionary law." Evolutionary Theory **1**: 1 - 30.

Vardi, A., L. Haramaty, et al. (2012). "Host-virus dynamics and subcellular controls of cell fate in a natural coccolithophore population." PNAS.

Vardi, A., B. A. Van Mooy, et al. (2009). "Viral Glycoshpingolipids Induce Lytic Infection and Cell Death in Marine Phytoplankton." Science **326**: 861-865.

Vardi, A., B. A. Van Mooy, et al. (2009). "Viral Glycosphingolipids Induce Lytic Infection and Cell Death in Marine Phytoplankton." Science **326**: 861 - 865.

Wilson, W. H., D. C. Schroeder, et al. (2005). "Complete genome sequence and lytic phase transcription profile of a Coccolithovirus." Science **309**: 1090 - 1092.

Xu, C. and J. Min (2011). "Structure and function of WD40 domain proteins." Protein Cell **2**(3): 202 - 214.

Zeng, L. R., C. H. Park, et al. (2008). "Classification, expression pattern, and E3 ligase activity assay of rice U-box-containing proteins." Molecular Plant **1**(5): 800 - 815.

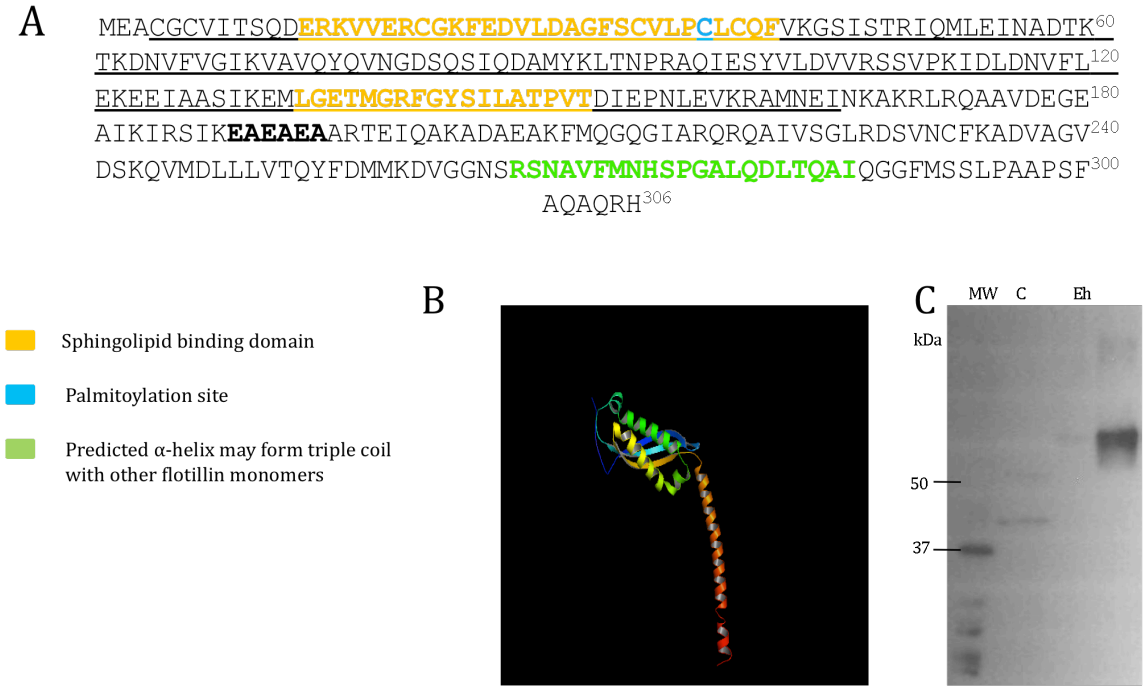

Figure 1.1: Analysis of a flotillin-like protein in *Emiliania huxleyi* CCMP strain 1516. (A) We identified a 306 amino acid, 33.5 kDa flotillin-like protein within the sequenced genome of *E. huxleyi* strain 1516 (Protein ID 363433), that contains notable lipid raft-associated domain characteristics. Predicted secondary structural elements of the putative *E. huxleyi*flotillin show the evolutionary conserved ProhibitinHomology(PHB)/StomatinProhibitinFlotillin Homology(SPFH) domain residues (aa 4 – 166; underlined), which are normally characteristic of lipid rafts in higher eukaryotes. The hydrophobic Sphingolipid Binding Domain (SBD) regions (aa 13-41; aa 133-151), along with the conserved palmitoylation site, contribute to membrane association where an α-helix coil is predicted to form dimers with other flotillin molecules. (B) Tertiary structure prediction of the *E. huxleyi* putative flotillin sequence (Phyre2 PDB SCOP code c3bk6C membrane protein; viewed with PyMOL software), with visualization of a predicted α-helix coil dimerizing tail (orange-red). (C) Western blot analysis of *E. huxleyi* cell extracts with a human anti-flotillin antibody displayed strong immunohybridization with a 67 kDa protein in *E. huxleyi* 1516 consistent with the predicted size of a dimerizedflotillin-like protein. Flotillin control immunoblot analysis with human A-375 whole cell lysate of malignant melanoma cells recognized the predicted 42 kDa human flotillin (NCBI Accession #AAF17215; 253 aa). Molecular weight markers (MW) are indicated.

A

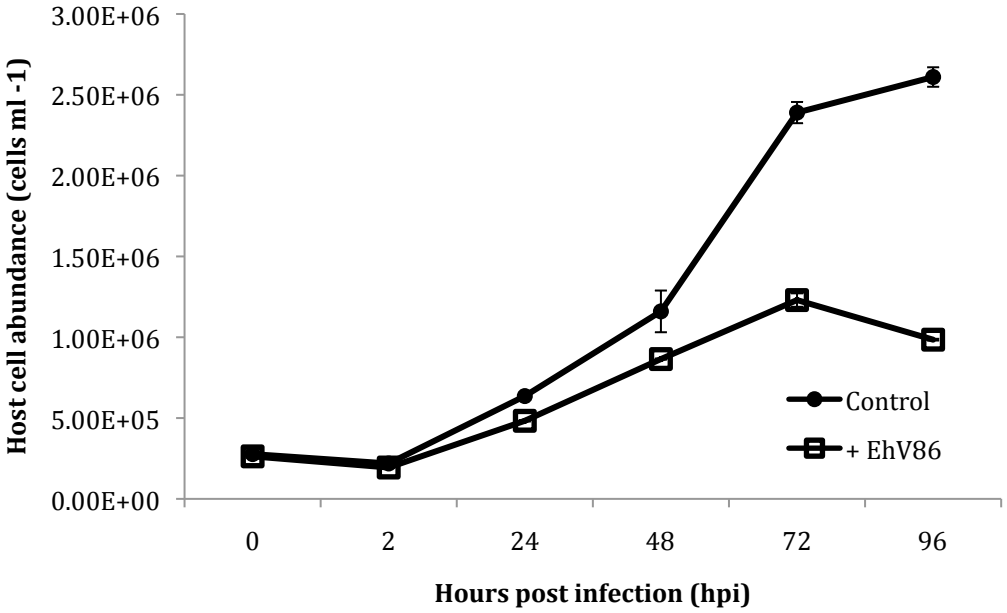

B

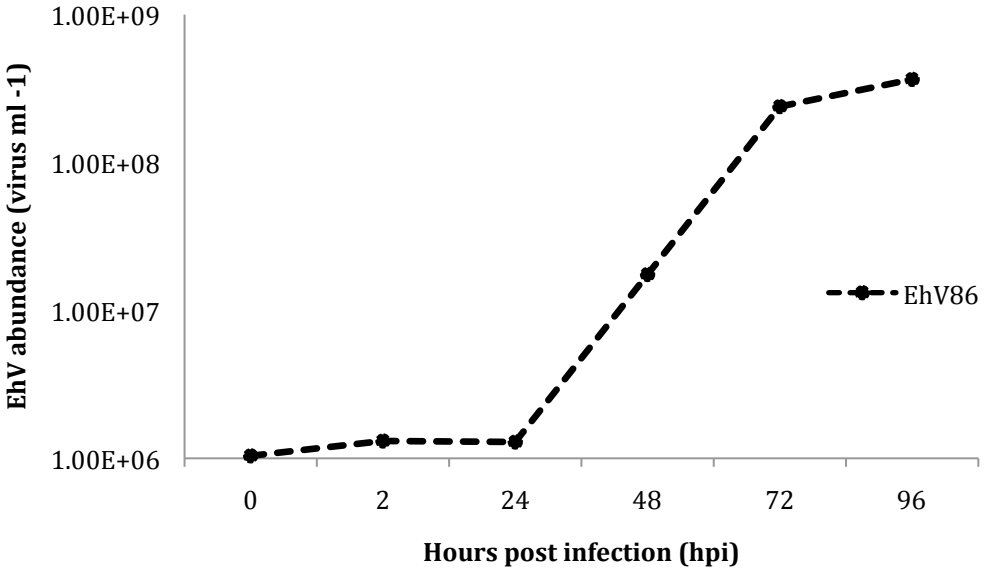

Figure 1.2: Dynamics of EhV86 infection of *Emiliania huxleyi* CCMP strain 1516. Time course of host (A) and virus (B) abundance over 96 hours for EhV86 infected (+EhV86) and uninfected control (control) cultures. Error bars represent standard deviation for triplicate measurements and, where not discernible, are smaller than symbol size.

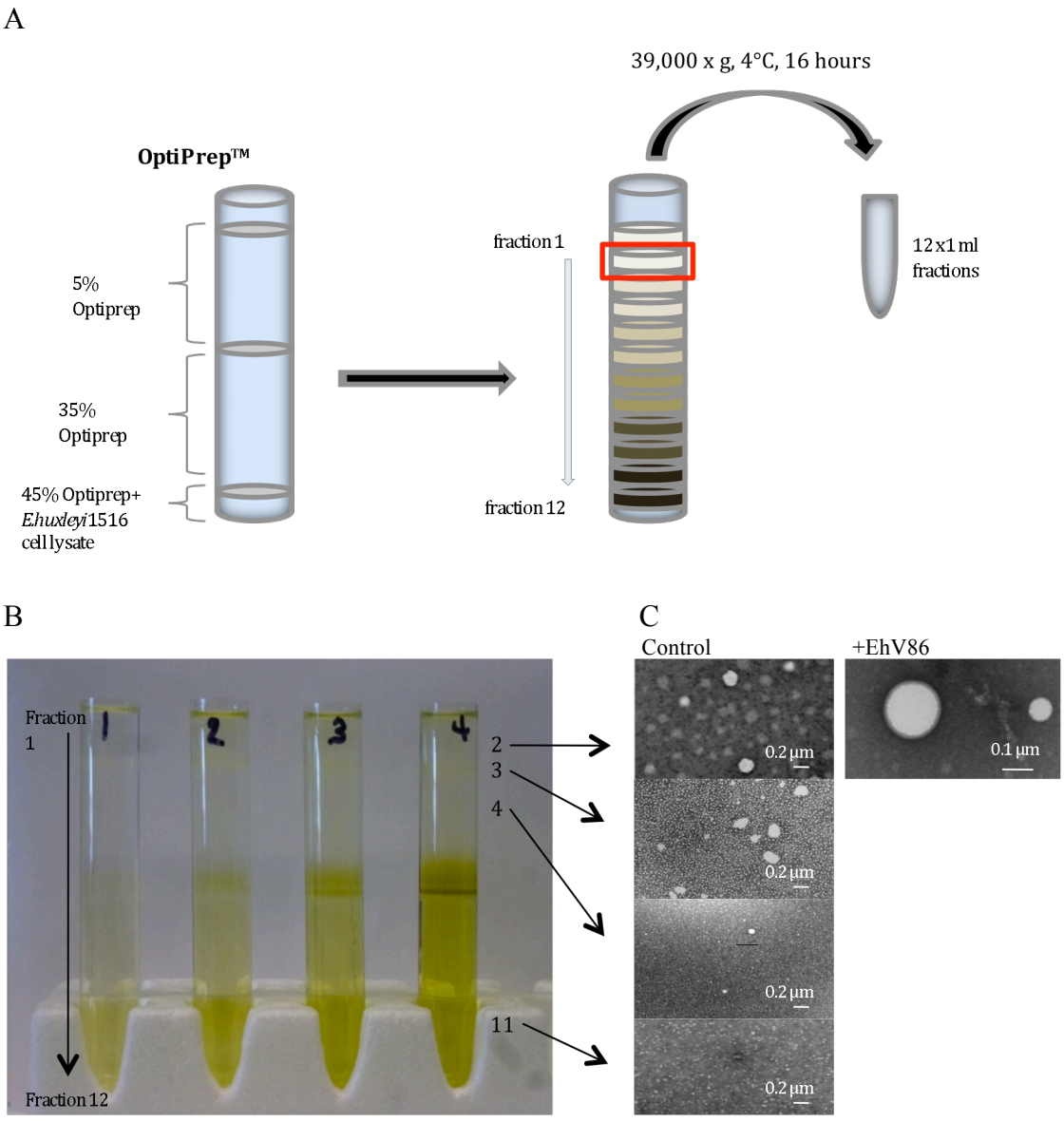

Figure 1.3: Lipid raft isolation and characterization in *Emiliania huxleyi* strain 1516. (A) Schematic of the OptiPrep density gradient technique and procedure used to isolate lipid raft fractions. Fraction 2 (red box) highlights lipid raft fraction. (B) Picture of OptiPrep gradients corresponding to the 2 (#1), 24 (#2), 48 (#3), and 72 (#4) hour samples for control *E. huxleyi* strain 1516. Gradients were also performed for EhV86-infected cells at same time points (not shown). (C) Direct visualization of lipid vesicles in select fractions (indicated by arrows) via transmission electron microscopy (TEM). Images in the left column correspond to uninfected control cells; image in right column corresponds to fraction 2 for EhV86-infected-cells. Note the presence of prominent detergent resistant lipid vesicles only in Fractions 2 and 3. No lipid vesicles were observed in lower fractions for either treatment.

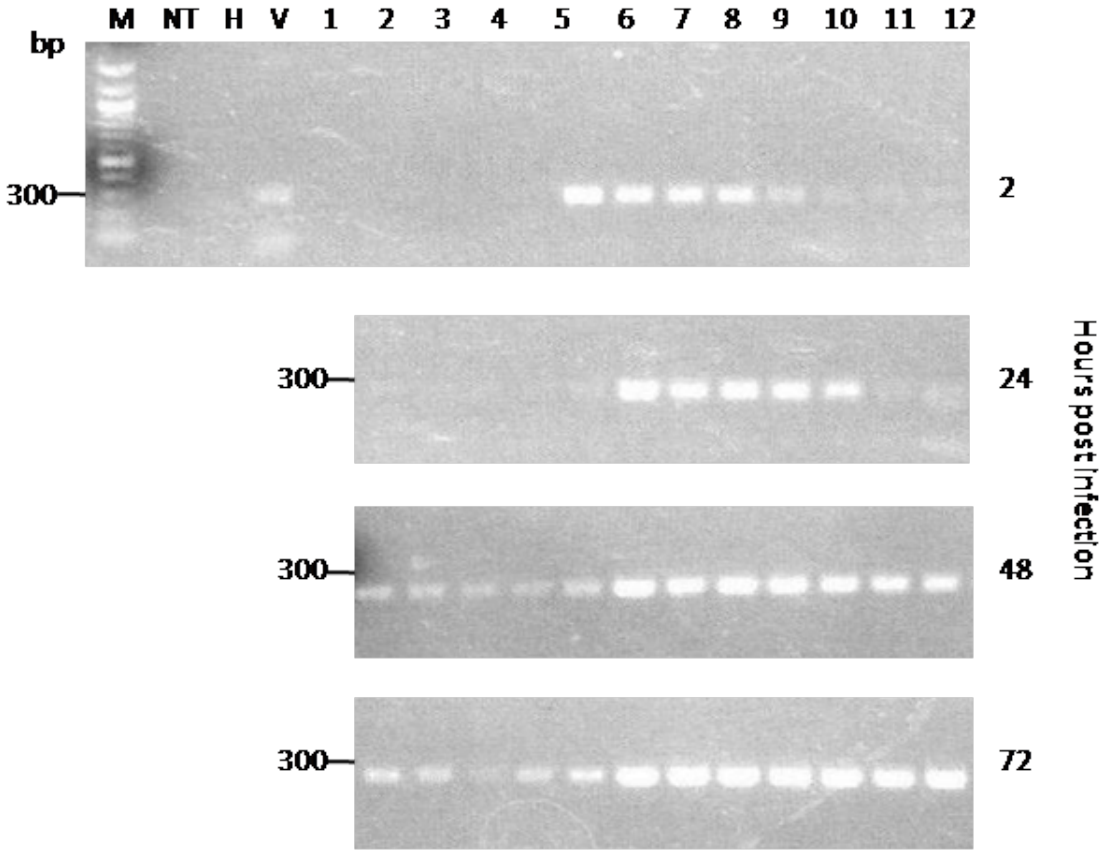

Figure 1.4: Distribution of EhVs in OptiPrep density gradients. Polymerase chain reaction (PCR) of the EhV major capsid protein (MCP; see methods) was used as a proxy to identify the distribution of EhVs (and associated DNA) in density gradients of EhV86-infected cell fractions for 2, 24, 48 and 72 hour post infection samples. Successful amplification of the expected 248 base pair amplicon was detected in fractions for each time point. Note that at early time points (2 – 24 hours), MCP was distributed between fractions 6 – 10. Subsequent time points (48 and 72 hours) displayed intense amplificons in Fractions 6 – 12 and weakeramplification in Fractions 1 – 5; this corresponded with 10- to 100-fold increase in EhV abundance (See Figure 1.1B). EhV86 viral lysate served as a positive control (lane 4, 'V'; upper panel). No template (NT) and genomic DNA for *Emiliania huxleyi* CCMP strain 373 were used as negative controls (lane 2 and 3 respectively; upper panel). Molecular weight (bp) markers are indicated.

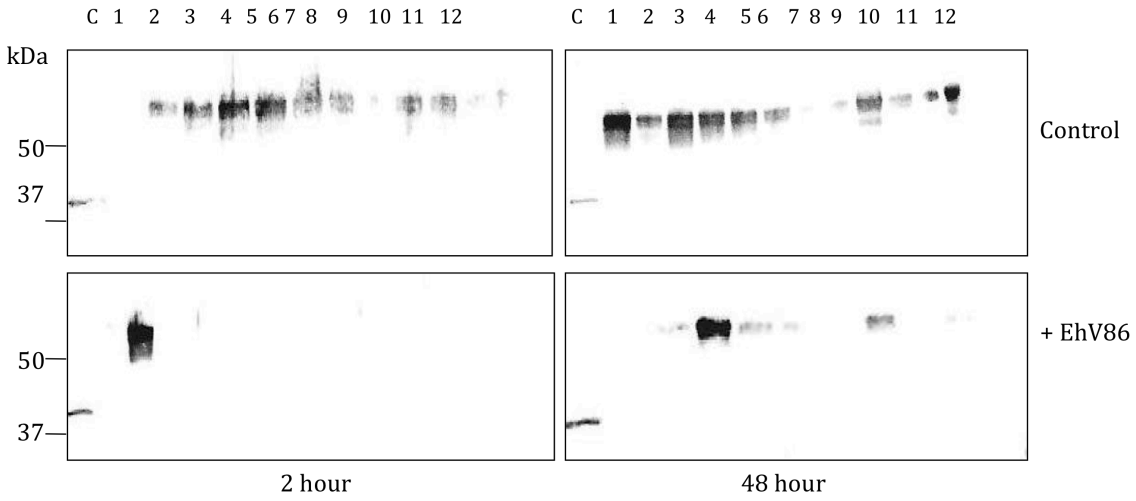

Figure 1.5: Distribution of the *E. huxleyi* flotillin-like protein in OptiPrep density gradients. Anti-flotillin Western immunoblot analysis of density gradient fractions at 2 and 48 hours for uninfected (control; top row) and EhV86-infected (+EhV86; bottom row) cells. Note that, while the prominent flotillin-like protein is distributed among most control fractions, it is concentrated within fractions 1 – 5. In contrast, EhV86-infection considerably narrows this protein to within fractions 2 – 3. Flotillin control immunoblot analysis recognized the predicted 42 kDa human flotillin (NCBI Accession# AAF17215; 253 aa) in human A-375 whole cell lysate of malignant melanoma cells. Molecular weight markers (MW) are indicated.

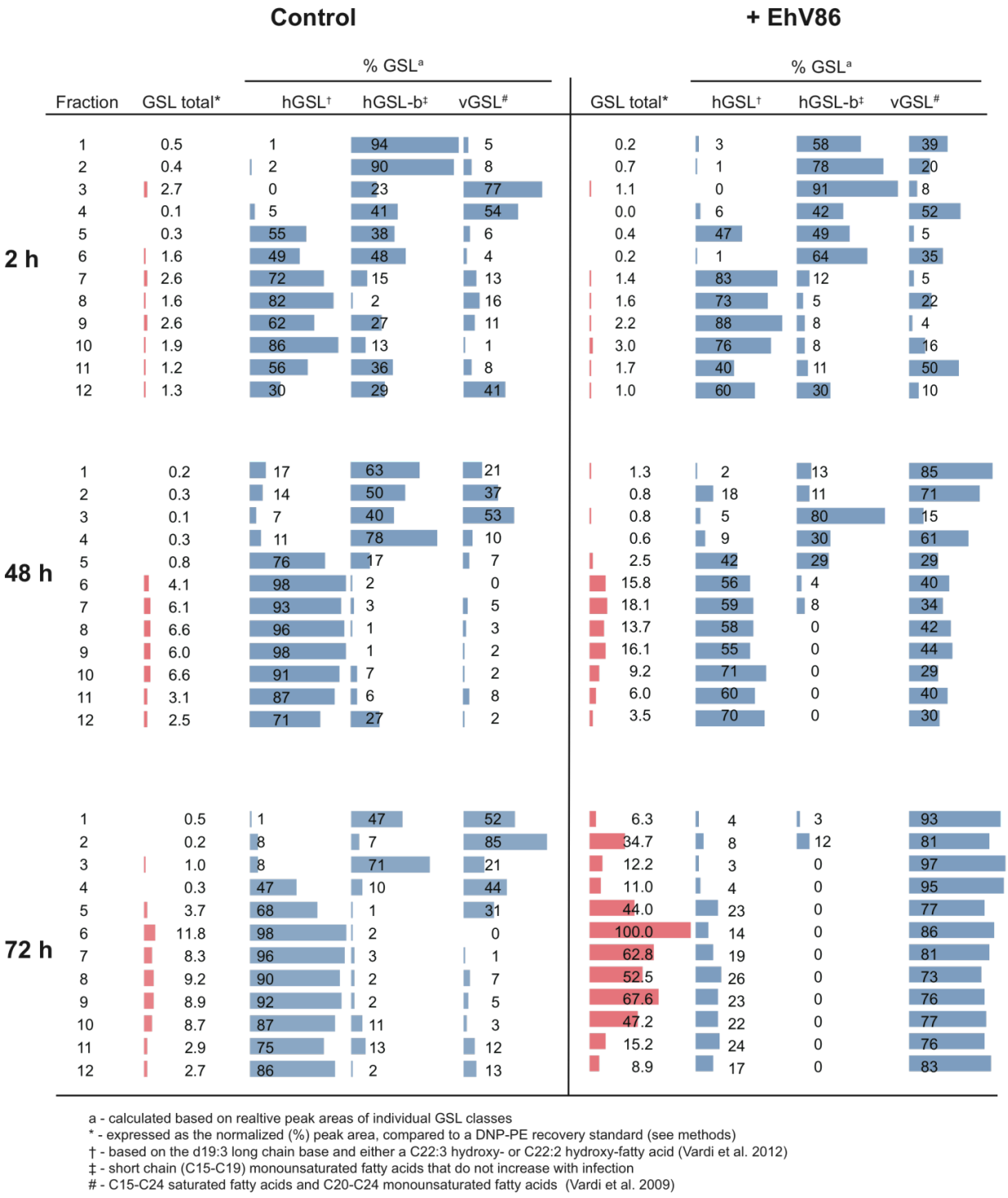

Figure 1.6: Distribution of total glycosphingolipids (GSLs) and the corresponding relative percentages of individual GSL classes (hGSL, hGSL-b, and vGSL) in OptiPrep density gradient fractions (1-12) for uninfected control and EhV86-infected *Emiliania huxleyi* at 2, 48 and 72 h post infection.

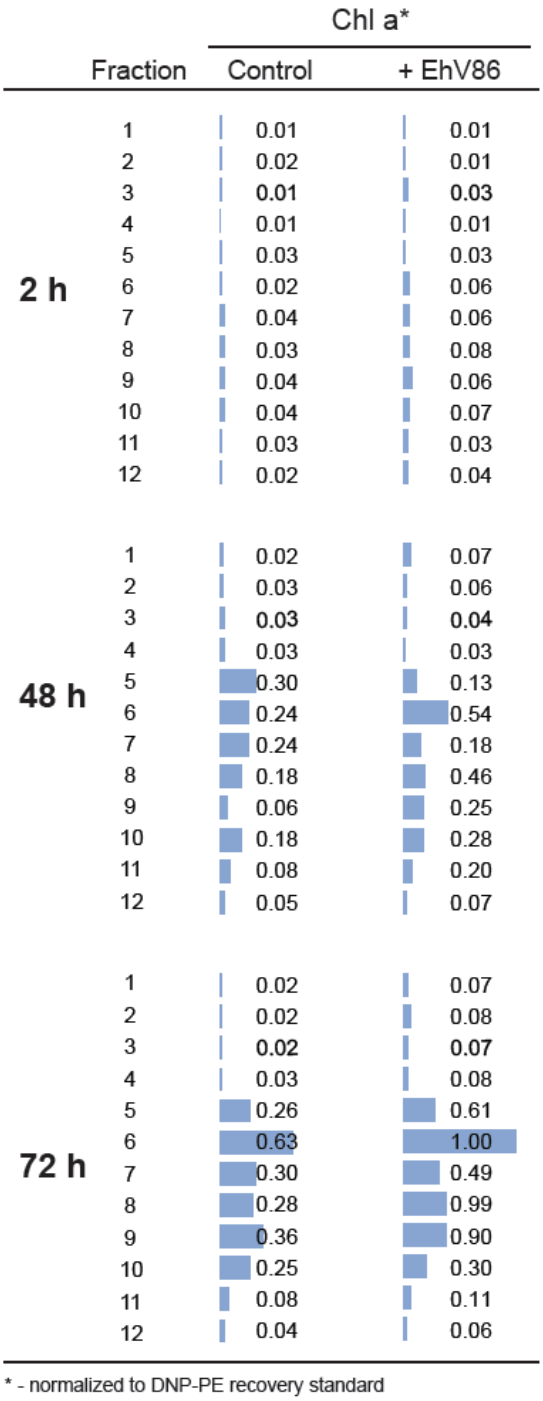

Figure 1.7: Chlorophyll a distribution in OptiPrep density gradient fractions (1-12) for uninfected control and EhV86-infected *Emiliania huxleyi* at 2, 48 and 72 h post infection.

Table 1.1: Detailed breakdown of the distribution of hGSL-b‡ and vGSL# species in OptiPrep density gradients for uninfected *E. huxleyi*

Fatty Acid			C24:0	C23:0	C22:0	C21:0	C20:0	C19:0	C18:0	C17:0	C16:0	C15:0		C24:1	C23:1	C22:1	C21:1	C20:1	C19:1	C18:1	C17:1	C16:1	C15:1	
m/z			832	*818	*804	790	776	762	748	*734	720	706	total	*830	816	802	788	774	760	746	732	718	704	total
Sample	Time	**Fraction**	relative amount normalized to DNP-PE																					
Ehux1516 control	2 h	1	0.00	0.00	0.00	0.00	0.00	0.00	0.00	0.00	0.00	0.00	0.00	0.00	0.00	0.00	0.00	0.00	0.00	0.00	0.00	0.02	0.00	0.03
		2	0.00	0.00	0.00	0.00	0.00	0.00	0.00	0.00	0.00	0.00	0.00	0.00	0.00	0.00	0.00	0.00	0.00	0.00	0.02	0.00	0.00	0.02
		3	0.00	0.00	0.00	0.00	0.00	0.00	0.12	0.00	0.00	0.00	0.12	0.00	0.00	0.00	0.00	0.00	0.00	0.00	0.03	0.00	0.00	0.04
		4	0.00	0.00	0.00	0.00	0.00	0.00	0.00	0.00	0.00	0.00	0.00	0.00	0.00	0.00	0.00	0.00	0.00	0.00	0.00	0.00	0.00	0.00
		5	0.00	0.00	0.00	0.00	0.00	0.00	0.00	0.00	0.00	0.00	0.00	0.00	0.00	0.00	0.00	0.00	0.00	0.00	0.00	0.00	0.00	0.01
		6	0.00	0.00	0.00	0.00	0.00	0.00	0.00	0.00	0.00	0.00	0.00	0.00	0.00	0.00	0.00	0.00	0.00	0.02	0.02	0.01	0.00	0.04
		7	0.00	0.00	0.01	0.00	0.00	0.00	0.00	0.00	0.01	0.00	0.02	0.00	0.00	0.00	0.00	0.00	0.00	0.01	0.00	0.00	0.01	0.02
		8	0.00	0.00	0.00	0.00	0.00	0.00	0.00	0.00	0.00	0.00	0.01	0.00	0.00	0.00	0.01	0.00	0.00	0.00	0.00	0.00	0.00	0.01
		9	0.00	0.00	0.00	0.00	0.00	0.00	0.00	0.00	0.00	0.00	0.00	0.00	0.01	0.00	0.00	0.00	0.00	0.00	0.00	0.04	0.00	0.05
		10	0.00	0.00	0.00	0.00	0.00	0.00	0.00	0.00	0.00	0.00	0.00	0.00	0.00	0.00	0.00	0.00	0.00	0.00	0.00	0.01	0.00	0.02
		11	0.00	0.00	0.00	0.00	0.00	0.00	0.00	0.00	0.00	0.00	0.01	0.00	0.00	0.00	0.00	0.00	0.00	0.00	0.00	0.02	0.00	0.03
		12	0.03	0.00	0.00	0.00	0.00	0.00	0.00	0.00	0.00	0.00	0.03	0.00	0.00	0.00	0.00	0.00	0.00	0.00	0.01	0.00	0.00	0.02
	48 h	1	0.00	0.00	0.00	0.00	0.00	0.00	0.00	0.00	0.00	0.00	0.00	0.00	0.00	0.00	0.00	0.00	0.00	0.00	0.00	0.00	0.00	0.01
		2	0.00	0.00	0.00	0.00	0.00	0.00	0.00	0.00	0.00	0.00	0.00	0.00	0.00	0.00	0.00	0.00	0.00	0.00	0.00	0.00	0.00	0.01
		3	0.00	0.00	0.00	0.00	0.00	0.00	0.00	0.00	0.00	0.00	0.00	0.00	0.00	0.00	0.00	0.00	0.00	0.00	0.00	0.00	0.00	0.00
		4	0.00	0.00	0.00	0.00	0.00	0.00	0.00	0.00	0.00	0.00	0.00	0.00	0.00	0.00	0.00	0.00	0.00	0.01	0.01	0.00	0.00	0.01
		5	0.00	0.00	0.00	0.00	0.00	0.00	0.00	0.00	0.00	0.00	0.00	0.00	0.00	0.00	0.00	0.00	0.00	0.00	0.00	0.00	0.00	0.01
		6	0.00	0.00	0.00	0.00	0.00	0.00	0.00	0.00	0.00	0.00	0.00	0.00	0.00	0.00	0.00	0.00	0.00	0.00	0.00	0.00	0.00	0.01
		7	0.00	0.00	0.01	0.00	0.00	0.00	0.00	0.01	0.00	0.00	0.02	0.00	0.00	0.00	0.00	0.00	0.00	0.00	0.00	0.00	0.00	0.01
		8	0.00	0.00	0.00	0.01	0.00	0.00	0.00	0.00	0.00	0.00	0.01	0.00	0.00	0.00	0.00	0.00	0.00	0.00	0.00	0.00	0.00	0.01
		9	0.00	0.00	0.00	0.00	0.00	0.00	0.00	0.00	0.00	0.00	0.00	0.00	0.00	0.00	0.00	0.00	0.00	0.00	0.00	0.00	0.00	0.01
		10	0.00	0.00	0.00	0.00	0.00	0.00	0.00	0.00	0.00	0.00	0.01	0.00	0.00	0.00	0.00	0.00	0.00	0.02	0.00	0.00	0.00	0.03
		11	0.00	0.00	0.01	0.00	0.00	0.00	0.00	0.00	0.00	0.00	0.01	0.00	0.00	0.00	0.00	0.00	0.00	0.00	0.00	0.00	0.01	0.01
		12	0.00	0.00	0.00	0.00	0.00	0.00	0.00	0.00	0.00	0.00	0.00	0.00	0.00	0.00	0.00	0.00	0.02	0.00	0.00	0.01	0.00	0.04
	72 h	1	0.00	0.00	0.00	0.00	0.00	0.00	0.00	0.01	0.00	0.00	0.01	0.00	0.00	0.00	0.00	0.00	0.00	0.00	0.00	0.00	0.01	0.01
		2	0.00	0.00	0.00	0.00	0.00	0.00	0.00	0.00	0.00	0.00	0.00	0.00	0.01	0.00	0.00	0.00	0.00	0.00	0.00	0.00	0.00	0.01
		3	0.00	0.00	0.00	0.00	0.00	0.01	0.00	0.00	0.00	0.00	0.01	0.00	0.00	0.00	0.00	0.00	0.00	0.00	0.02	0.01	0.00	0.04
		4	0.01	0.00	0.00	0.00	0.00	0.00	0.00	0.00	0.00	0.00	0.01	0.00	0.00	0.00	0.00	0.00	0.00	0.00	0.00	0.00	0.00	0.00
		5	0.00	0.00	0.00	0.00	0.00	0.01	0.00	0.05	0.00	0.00	0.07	0.00	0.00	0.00	0.00	0.00	0.00	0.00	0.00	0.00	0.00	0.00
		6	0.00	0.00	0.00	0.00	0.00	0.00	0.00	0.00	0.00	0.00	0.00	0.00	0.00	0.00	0.00	0.00	0.00	0.00	0.00	0.00	0.01	0.01
		7	0.00	0.00	0.00	0.00	0.00	0.00	0.00	0.00	0.00	0.01	0.01	0.00	0.00	0.00	0.00	0.00	0.00	0.01	0.00	0.01	0.00	0.02
		8	0.00	0.00	0.04	0.00	0.00	0.00	0.00	0.00	0.00	0.00	0.04	0.00	0.00	0.00	0.00	0.00	0.00	0.00	0.00	0.01	0.00	0.01
		9	0.02	0.00	0.00	0.00	0.00	0.00	0.00	0.00	0.00	0.00	0.02	0.00	0.00	0.00	0.00	0.00	0.00	0.00	0.00	0.01	0.00	0.02
		10	0.00	0.00	0.00	0.00	0.00	0.00	0.01	0.00	0.00	0.00	0.01	0.00	0.00	0.00	0.00	0.00	0.00	0.02	0.02	0.00	0.01	0.06
		11	0.01	0.00	0.01	0.00	0.00	0.00	0.00	0.00	0.00	0.00	0.02	0.00	0.00	0.00	0.00	0.00	0.00	0.00	0.01	0.00	0.01	0.02
		12	0.00	0.01	0.00	0.00	0.00	0.00	0.00	0.00	0.00	0.00	0.02	0.00	0.00	0.00	0.00	0.00	0.00	0.00	0.00	0.00	0.00	0.01

‡- short chain (C15-C19) monounsaturated fatty acids that do not increase with infection

- C15-C24 saturated fatty acids and C20-C24 monounsaturated fatty acids (Vardi et al. 2009)

Table 1.2: Detailed breakdown of the distribution of hGSL-b‡ and vGSL# species in OptiPrep density gradients for EhV86-infected *E. huxleyi*

Fatty Acid			C24:0	C23:0	C22:0	C21:0	C20:0	C19:0	C18:0	C17:0	C16:0	C15:0		C24:1	C23:1	C22:1	C21:1	C20:1	C19:1	C18:1	C17:1	C16:1	C15:1	
m/z			832	*818	*804	790	776	762	748	*734	720	706	total	*830	816	802	788	774	760	746	732	718	704	total
Sample	Time	Fraction	relative amount normalized to DNP-PE																						
Ehux1516 + EhV86	2 h	1	0.00	0.00	0.00	0.00	0.00	0.00	0.00	0.00	0.00	0.00	0.00	0.00	0.00	0.00	0.00	0.00	0.00	0.01	0.00	0.00	0.00	0.01
		2	0.00	0.00	0.00	0.00	0.00	0.00	0.00	0.00	0.00	0.00	0.01	0.00	0.00	0.00	0.00	0.00	0.00	0.00	0.00	0.02	0.01	0.03
		3	0.00	0.00	0.00	0.00	0.00	0.00	0.00	0.00	0.00	0.00	0.00	0.00	0.00	0.00	0.00	0.00	0.00	0.04	0.00	0.01	0.01	0.06
		4	0.00	0.00	0.00	0.00	0.00	0.00	0.00	0.00	0.00	0.00	0.00	0.00	0.00	0.00	0.00	0.00	0.00	0.00	0.00	0.00	0.00	0.00
		5	0.00	0.00	0.00	0.00	0.00	0.00	0.00	0.00	0.00	0.00	0.00	0.00	0.00	0.00	0.00	0.00	0.00	0.00	0.00	0.00	0.00	0.01
		6	0.00	0.00	0.00	0.00	0.00	0.00	0.00	0.00	0.00	0.00	0.00	0.00	0.00	0.00	0.00	0.00	0.00	0.00	0.00	0.00	0.01	0.01
		7	0.00	0.00	0.00	0.00	0.00	0.00	0.00	0.00	0.00	0.00	0.00	0.00	0.00	0.00	0.00	0.00	0.00	0.00	0.01	0.00	0.00	0.01
		8	0.00	0.00	0.00	0.00	0.00	0.00	0.00	0.01	0.01	0.00	0.02	0.00	0.00	0.00	0.00	0.00	0.00	0.00	0.00	0.00	0.00	0.01
		9	0.00	0.00	0.00	0.00	0.00	0.00	0.00	0.00	0.00	0.00	0.00	0.00	0.00	0.00	0.00	0.00	0.00	0.00	0.00	0.00	0.00	0.01
		10	0.00	0.00	0.00	0.00	0.00	0.00	0.00	0.00	0.00	0.02	0.03	0.00	0.00	0.00	0.00	0.00	0.00	0.00	0.00	0.01	0.00	0.01
		11	0.00	0.00	0.00	0.00	0.00	0.05	0.00	0.00	0.00	0.00	0.05	0.00	0.00	0.00	0.00	0.00	0.00	0.00	0.00	0.00	0.00	0.01
		12	0.00	0.00	0.00	0.00	0.00	0.00	0.00	0.00	0.00	0.00	0.01	0.00	0.00	0.00	0.00	0.00	0.00	0.00	0.01	0.00	0.00	0.02
	48 h	1	0.00	0.00	0.01	0.00	0.00	0.00	0.00	0.00	0.00	0.00	0.02	0.04	0.00	0.00	0.00	0.00	0.00	0.00	0.00	0.00	0.00	0.05
		2	0.00	0.01	0.01	0.00	0.00	0.00	0.00	0.00	0.00	0.00	0.03	0.00	0.00	0.00	0.00	0.00	0.00	0.00	0.00	0.00	0.00	0.01
		3	0.00	0.00	0.00	0.00	0.00	0.00	0.00	0.00	0.00	0.00	0.01	0.00	0.00	0.00	0.00	0.00	0.01	0.00	0.01	0.01	0.01	0.04
		4	0.00	0.00	0.01	0.00	0.00	0.00	0.00	0.00	0.00	0.00	0.02	0.00	0.00	0.00	0.00	0.00	0.00	0.01	0.00	0.00	0.00	0.01
		5	0.00	0.01	0.03	0.00	0.00	0.00	0.00	0.00	0.00	0.00	0.04	0.00	0.00	0.00	0.00	0.00	0.03	0.01	0.00	0.00	0.00	0.05
		6	0.03	0.05	0.11	0.04	0.00	0.02	0.06	0.00	0.00	0.00	0.31	0.00	0.01	0.04	0.01	0.00	0.00	0.00	0.03	0.00	0.00	0.10
		7	0.01	0.02	0.05	0.05	0.00	0.00	0.03	0.00	0.00	0.00	0.16	0.00	0.01	0.08	0.10	0.00	0.00	0.00	0.00	0.08	0.00	0.27
		8	0.01	0.02	0.04	0.03	0.05	0.06	0.08	0.00	0.00	0.00	0.29	0.00	0.01	0.02	0.01	0.00	0.00	0.00	0.00	0.00	0.00	0.04
		9	0.00	0.03	0.05	0.04	0.01	0.02	0.01	0.01	0.01	0.00	0.19	0.00	0.02	0.14	0.05	0.00	0.00	0.00	0.00	0.00	0.00	0.22
		10	0.01	0.04	0.03	0.03	0.00	0.00	0.00	0.00	0.00	0.00	0.11	0.00	0.00	0.04	0.00	0.00	0.00	0.00	0.00	0.00	0.00	0.04
		11	0.00	0.01	0.02	0.00	0.00	0.05	0.00	0.00	0.00	0.00	0.10	0.00	0.00	0.02	0.00	0.02	0.00	0.00	0.00	0.00	0.00	0.04
		12	0.00	0.01	0.01	0.01	0.01	0.00	0.00	0.00	0.00	0.00	0.04	0.00	0.01	0.01	0.00	0.00	0.00	0.00	0.00	0.00	0.00	0.02
	72 h	1	0.04	0.07	0.03	0.08	0.00	0.00	0.02	0.01	0.00	0.00	0.26	0.00	0.03	0.02	0.03	0.00	0.00	0.00	0.00	0.01	0.00	0.08
		2	0.07	0.14	0.12	0.30	0.13	0.34	0.00	0.00	0.00	0.00	1.11	0.00	0.12	0.27	0.11	0.01	0.00	0.00	0.23	0.00	0.00	0.74
		3	0.03	0.07	0.06	0.10	0.01	0.02	0.01	0.00	0.00	0.00	0.31	0.00	0.10	0.15	0.13	0.00	0.00	0.00	0.00	0.00	0.00	0.37
		4	0.02	0.03	0.12	0.18	0.00	0.00	0.00	0.00	0.00	0.00	0.36	0.00	0.02	0.03	0.19	0.00	0.00	0.00	0.00	0.00	0.00	0.25
		5	0.11	0.21	0.34	0.21	0.36	0.01	0.00	0.03	0.00	0.02	1.28	0.12	0.12	0.22	0.22	0.00	0.00	0.00	0.00	0.00	0.00	0.68
		6	0.35	0.86	1.00	0.56	0.19	0.33	0.24	0.13	0.00	0.01	3.69	0.08	0.32	0.45	0.38	0.04	0.01	0.00	0.00	0.00	0.00	1.29
		7	0.12	0.31	0.44	0.38	0.13	0.40	0.01	0.01	0.00	0.03	1.84	0.05	0.26	0.31	0.33	0.15	0.00	0.00	0.00	0.00	0.00	1.10
		8	0.15	0.35	0.38	0.27	0.05	0.12	0.04	0.01	0.01	0.01	1.38	0.06	0.21	0.34	0.20	0.02	0.00	0.00	0.00	0.00	0.00	0.84
		9	0.15	0.40	0.52	0.41	0.15	0.15	0.07	0.03	0.01	0.01	1.90	0.09	0.23	0.44	0.31	0.01	0.00	0.00	0.00	0.00	0.00	1.08
		10	0.08	0.20	0.36	0.30	0.10	0.10	0.15	0.00	0.04	0.00	1.33	0.02	0.17	0.27	0.26	0.06	0.00	0.00	0.00	0.00	0.00	0.78
		11	0.03	0.08	0.13	0.10	0.01	0.01	0.06	0.00	0.00	0.00	0.42	0.01	0.06	0.10	0.08	0.00	0.00	0.00	0.00	0.00	0.00	0.24
		12	0.02	0.04	0.09	0.07	0.01	0.00	0.01	0.00	0.00	0.00	0.25	0.00	0.04	0.09	0.05	0.00	0.00	0.00	0.00	0.00	0.00	0.18

*m/z 830, 818, 804, 734 were included in the supplementary material of Vardi et al., 2009.

‡- short chain (C15-C19) monounsaturated fatty acids that do not increase with infection

- C15-C24 saturated fatty acids and C20-C24 monounsaturated fatty acids (Vardi et al. 2009)

Table 1.3: Top 20 protein hits[#] from proteomic analysis of lipid rafts[‡] for uninfected *Emiliania huxleyi* strain 1516 at 2 hours

Protein ID*	Protein description	Protein log e	Count of unique peptides	Protein MW
444491	Outer membrane protein porin	-160.6	19	31.6
363433	Band_7; flotillin-like protein	-109.1	14	33.5
444671	Protein of unknown function	-73.5	11	19.6
366130	Chlorophyll a/b binding protein	-72.4	9	20.2
432658	Import receptor subunit	-67	7	30.9
440685	High affinity nitrate transporter	-61.1	9	73.3
436031	Delta-carbonic anhydrase	-58.9	8	72.4
446310	Chlorophyll a/b binding protein	-58.2	6	22.6
441334	Type 1 actin, partial	-56.2	8	41.6
358662	Chlorophyll a/b binding protein	-55.9	5	21.9
420185	Chlorophyll a/b binding protein	-53.1	3	15.6
433847	Chlorophyll a/b binding protein	-53	7	30
360139	Substrate carrier	-49.9	6	36.7
246130	Histone H4	-46.8	7	11.4
439254	Formate/nitrite transporter	-35.5	5	29.3
46509	Chlorophyll a/b binding protein	-35.2	5	18
434557	Protein of unknown function	-31.8	4	16.5
444211	Protein of unknown function	-27.8	4	30.6
460471	Protein of unknown function	-26.8	4	31.2
447939	Sodium/calcium exchanger membrane region	-19.8	3	67.9

* JGI (filtered best models; http://genome.jgi-psf.org/)
# - based on rank order of Protein log e
‡ - fraction #2

Table 1.4: Top 20 protein hits[#] from proteomic analysis oflipid rafts[‡] for EhV86-infected *Emiliania huxleyi* cells at 2 hours post infection

Protein ID*	Protein description	Protein log e	Count of unique peptides	protein MW
444491	Outer membrane protein porin	-160.6	19	31.6
363433	Band_7; flotillin-like protein	-109.1	14	33.5
444671	Protein of unknown function	-73.5	11	19.6
366130	Chlorophyll a/b binding protein	-72.4	9	20.2
439740	Membrane bound proton transporter	-71.2	9	93.7
432658	Import receptor subunit	-67	7	30.9
442092	Heat Shock Protein (HSP) 70	-62	9	71.8
440685	High affinity nitrate transporter	-61.1	9	73.3
437063	Carrier protein	-59.8	7	33.3
436031	Delta-carbonic anhydrase; ca+ ion binding	-58.9	8	72.4
446310	Chlorophyll a/b binding protein	-58.2	6	22.6
441334	Type 1 actin, partial	-56.2	8	41.6
358662	Chlorophyll a/b binding protein	-55.9	5	21.9
420185	Chlorophyll a/b binding protein	-53.1	3	15.6
433847	Chlorophyll a/b binding protein	-53	7	30
360139	Substrate carrier	-49.9	6	36.7
246130	Histone H4	-46.8	7	11.4
439254	Formate/nitrite transporter	-35.5	5	29.3
46509	Chlorophyll a/b binding protein	-35.2	5	18
75032	H+ pyrophosphatase	-32.9	5	75.8

* JGI (filtered best models; http://genome.jgi-psf.org/)
# - based on rank order of Protein log e
‡ - fraction #2

Table 1.5: List of unique proteins[#] from proteomic analysis of lipid rafts[‡] for control *Emiliania huxleyi* cells with a putative role in innate immunity, signal transduction and death pathways

Protein ID*	Protein description	protein log e	count of unique peptides	protein MW
440685	Crystallin_betagamma	-61.1	9	73.3
439254	Formate/nitrite transporter	-35.5	5	29.3
64600	Formate/nitrite transporter	-13.6	2	30.9
116083	DNA-binding SAP	-8.2	2	83.1
448295	Ankyrin	-6.6	2	360.8
445748	Histone H2A	-2.9	1	13.6
463505	SANT, DNA-binding	-2.3	1	141.6
453318	Peptidase, cysteine peptidase active site	-2.3	1	117.1
450438	Phox-like	-2	1	106.5
56408	AAA ATPase core	-1.8	1	21
449479	Nitrilehydratase alpha chain	-1.8	1	52.1
236447	NUDIX hydrolase	-1.6	1	36.4
204524	Esterase	-1.6	1	29.5
457010	UvrB/UvrC protein	-1.6	1	33.3
460651	Sec31-like secretory protein (WD40 containing)	-1.6	1	33.2
205013	Fibronectin, type III	-1.5	1	198.2
212473	TPR repeat	-1.4	1	68
350674	Protein kinase-like	-1.4	1	10.5
210405	WW/Rsp5/WWP	-1.4	1	39
450932	Ankyrin	-1.3	1	43.2
255657	Peptidase M24	-1.3	1	18.9
468714	Patatin	-1.3	1	34.6
450457	Ankyrin	-1.3	1	70
236138	K+ channel tetramerisation	-1.3	1	81
115688	HEAT repeat, intracellular transport	-1.3	1	168.3
415400	Thioredoxin	-1.3	1	27.8
228098	Protein phosphatase 2C-like	-1.2	1	19.5
109218	Ferredoxin	-1.1	1	125.8
461763	Nucleoporin interacting component	-1.1	1	69.1
203844	U Box	-1.1	1	16.9
428651	Leucine carboxyl methyl transferase	-1.1	1	37.2

*JGI (filtered best models; http://genome.jgi-psf.org/)
- proteins were not found in the corresponding EhV86-infected *E.huxleyi* cell samples at same time point and fraction.
‡ - fraction #2 from 2 h

Table 1.6: List of proteins[#] of unknown functions from proteomic analysis of lipid rafts[‡] for healthy control *Emiliania huxleyi* cells at 2 hours

Protein ID*	Protein description	protein log e	count of unique peptides	protein MW
235383	Protein of unknown function	-6.2	2	79.5
352050	Protein of unknown function	-3.9	1	38.7
437040	Protein of unknown function	-2.5	1	89.5
465597	Protein of unknown function	-2.2	1	168.2
446322	Protein of unknown function	-2.2	1	64.4
197272	Protein of unknown function	-2.1	1	35.3
236194	Protein of unknown function	-1.9	1	24.8
206208	Protein of unknown function	-1.8	1	51.1
355011	Protein of unknown function	-1.7	1	94
354217	Protein of unknown function	-1.7	1	12.3
195735	Protein of unknown function	-1.5	1	44.1
455798	Protein of unknown function	-1.5	1	40
102429	Protein of unknown function	-1.5	1	70.3
201998	Protein of unknown function	-1.5	1	38.4
373055	Protein of unknown function	-1.4	1	11.8
121199	Protein of unknown function	-1.3	1	45.9
120799	Protein of unknown function	-1.3	1	25.9
457131	Protein of unknown function	-1.2	1	47.7
249414	Protein of unknown function	-1.1	1	51.1

*JGI (filtered best models; http://genome.jgi-psf.org/)
- proteins were not found in the corresponding uninfected control sample at same time point and fraction.
‡ - fraction #2 from 2 h

Table 1.7: List of unique proteins[#] from proteomic analysis of lipid rafts[‡] for EhV86-infected *Emiliania huxleyi* cells at 2 hours post infection with a putative role in innate immunity, signal transduction, and death pathways

Protein ID*	Protein description	Protein log e	Count of unique peptides	Protein MW
436974	Lipase	-4.7	1	36.5
111458	Ubiquitin-associated protein	-3.4	1	122.7
468259	2OG-FeII oxygenase	-2.2	1	79.8
449765	Protein kinase	-1.9	1	93.9
434687	Aldehydedehydrogenase	-1.9	1	25.7
442793	Sodium solute transporter	-1.9	1	67
363731	HUS-1 DNA clamp	-1.8	1	35.8
117293	Phospholipid/glycanolacyltransferase	-1.7	1	60.1
351398	Ribose-5 phosphate isomerase	-1.7	1	28.4
Q4A2Y5	C type lectin 1 domain–containing membrane protein (EhV149)	-1.7	1	31.1
459348	DENN/MADD	-1.7	1	72
442619	Sigma 70	-1.5	1	33
448030	Aspartyl/Asparaginyl beta-hydroxylase	-1.4	1	49.9
105335	Forkhead; FHA	-1.4	1	144.1
459716	EGF; CUB domain	-1.4	1	154.5
218568	AAA ATPase	-1.4	1	91.6
212522	Hairpin loop containing domain	-1.3	1	47.9
53698	WD40-containing U5 snRNP-specific protein	-1.3	1	31.2
196637	FHA-domain	-1.3	1	56.8
416208	Ribosomal L17	-1.3	1	15.8
443600	PRICHEXTENSN	-1.2	1	47.7
110078	Ca+ binding EF-hand	-1.2	1	30.3
196713	RCCI	-1.2	1	51.4
226966	Amino acid/polyamine transporter	-1.2	1	37.6
56428	Pseudouridinesynthase	-1.2	1	23.6
114838	Leucine-rich repeat (LRR-RI)	-1.2	1	52.6
451621	JmjC	-1.1	1	84.9
373476	Zinc finger, PHD-type	-1.1	1	13.6
466323	TIR	-1.1	1	193.3
439552	Naringenin-chalconesynthase	-1.1	1	68.2
235877	PbH1	-1.1	1	64.9
420913	B56-pyrophosphatase	-1.1	1	50.5
449182	CRAL/TRIO domain containing protein	-1.1	1	42.4
246386	Glycosyltransferase	-1.1	1	68.7

*JGI (filtered best models; http://genome.jgi-psf.org/)
- proteins were not found in the corresponding uninfected control sample at same time point and fraction.
‡ - fraction #2 from 2 h

Table 1.8: List of proteins[#] of unknown function from proteomic analysis of lipid rafts[‡] for EhV86-infected *E. huxleyi* cells at 2 hours post infection

Protein ID*	Protein description	Protein log e	Count of unique peptides	Protein MW
444671	Protein of unknown function	-73.5	11	19.6
434557	Protein of unknown function	-31.8	4	16.5
444211	Protein of unknown function	-27.8	4	30.6
457279	Protein of unknown function	-27.2	4	22.8
460471	Protein of unknown function	-26.8	4	31.2
433714	Protein of unknown function	-16.2	3	38.3
438689	Protein of unknown function	-13.2	2	46.8
79680	Protein of unknown function	-11.5	2	41.5
445900	Protein of unknown function	-11.4	2	24.4
123369	Protein of unknown function	-7.9	1	13
438676	Protein of unknown function	-7.2	1	64.4
445358	Protein of unknown function	-6.6	1	31.4
243041	Protein of unknown function	-6.2	1	70.4
351234	Protein of unknown function	-2.5	1	42
204511	Protein of unknown function	-2.2	1	21.3
248575	Protein of unknown function	-2.2	1	56.6
462088	Protein of unknown function	-2.1	1	231.9
118703	Protein of unknown function	-2	1	41
464162	Protein of unknown function	-2	1	112.9
244446	Protein of unknown function	-1.9	1	59.6
468885	Protein of unknown function	-1.6	1	58.1
461383	Protein of unknown function	-1.6	1	25.8
246261	Protein of unknown function	-1.5	1	35.5
228791	Protein of unknown function	-1.5	1	16.1
250675	Protein of unknown function	-1.5	1	13.9
207368	Protein of unknown function	-1.5	1	78.5
115025	Protein of unknown function	-1.5	1	50.8
457317	Protein of unknown function	-1.5	1	28.4
461703	Protein of unknown function	-1.4	1	155.5
118788	Protein of unknown function	-1.4	1	62.6
466422	Protein of unknown function	-1.4	1	58.2
120840	Protein of unknown function	-1.3	1	28.2
420286	Protein of unknown function	-1.2	1	24.5
434923	Protein of unknown function	-1.2	1	29.5
222639	Protein of unknown function	-1.2	1	20
219116	Protein of unknown function	-1.1	1	27.9
98319	Protein of unknown function	-1.1	1	159.6
116543	Protein of unknown function	-1.1	1	109.9
463909	Protein of unknown function	-1.1	1	33

*JGI (filtered best models; http://genome.jgi-psf.org/)
- proteins were not found in the corresponding uninfected control sample at same time point and fraction.
‡ -fraction #2 from 2 h